Innov. Infrastruct. Solut. (2017) 2:34
DOI 10.1007/s41062-017-0086-3

TECHNICAL PAPER

Getting high-quality samples in 'sensitive' soils for advanced laboratory tests

António Viana da Fonseca[1] · **Jubert Pineda**[2]

Received: 11 April 2017 / Accepted: 2 June 2017 / Published online: 26 June 2017

Abstract Laboratory tests are well recognized as highly appropriate for defining the engineering properties of geomaterials, in terms of constitutive law parameters for modeling geotechnical engineering problems. The strong development of advanced techniques, both in equipment and in data interpretation, has increased the confidence in laboratory testing, while on the other hand the limitations due to the quality of soil sampling with depth and the spatial representativeness of the samples are less consensual. Still, the development of new methods for assuring high-quality samples is increasing, together with sampling quality assessment by non-destructive methods using vibration wave velocities. Interpretation methods of in situ tests for ground characterization have also evolved significantly, increasing the reliability of these methods. Their versatility to cover large areas on site and the fact that these tests are, in principle, performed at the actual state (physical and stress) conditions, as well as the improvements in the correlations between field tests and hydraulic and geomechanical parameters, allow joining the quality of data and theoretical approaches, namely through critical state soil mechanics. This keynote paper discusses some of the aspects that can and should enable the association of ground characterization from laboratory testing over undisturbed samples used in more or less advanced tests, enhancing the determinant conditioning factor, that is, the sampling technique to get representative specimens and the way this is assessed. The confidence that we expect to have on the geomechanical parameters that we need for our geotechnical activities will mostly depend on this in view of the high uncertainties of the parametrical correlations with in situ test data, therefore, important in ground characterization. This is especially relevant in sensitive soils, such as soft fine soils, loose sandy soils, or young residuals soils. These have or can have "weak" equilibria of the interparticle micro- and macrostructures (or their arrangement, fabric) that will change substantially their properties if samples are collected and conditioned with processes that do not preserve that intrinsic "ADN". The change in these natural conditions can be evaluated by techniques of quality assessment, which will be discussed in what follows.

Keywords In situ and laboratory test · Sampling quality · Non-destructive methods

Introduction

Geotechnical sampling is aimed to obtain soil specimens for laboratory characterization which is typically composed of three classes of laboratory tests. The first class corresponds to characterization/identification tests devoted to establish physical and chemical soil composition (e.g., particle size distributions and XRD analysis). Tests carried out to determine soil state variables such as porosity, degree of saturation, fabric (geometric distribution of grains, aggregates and cement), as well as total stresses and pore water pressure comprise the second class of laboratory tests. The third class

This paper was selected from GeoMEast 2017—Sustainable Civil Infrastructures: Innovative Infrastructure Geotechnology.

✉ António Viana da Fonseca
viana@fe.up.pt

Jubert Pineda
jubert.pineda@newcastle.edu.au

[1] CONSTRUCT-GEO–Faculty of Engineering of University of Porto, Porto, Portugal

[2] University of Newcastle, Newcastle, NSW, Australia

includes mechanical (element) tests performed to estimate mechanical properties such as strength, stiffness, compressibility, and permeability. In all cases, tested specimens must preserve similar composition and state to the in situ soil to obtain representative index and mechanical parameters to be used in geotechnical design.

The early work by Hvorslev [27] summarized the current practice of subsurface exploration and sampling of soils for engineering purposes. He recognized the difficulties for obtaining high-quality soil specimens and suggested comprehensive guidelines for selecting samplers for soils and rocks. Although important advances in soil sampling techniques occurred after its publication, the report published by Hvorslev [27] is still nowadays the reference for several standards and guidelines worldwide. In the case of soft cohesive soils, updated guidelines were proposed in the International Manual for sampling of soft cohesive soils [29], edited by the subcommittee on Soil Sampling of the ISSMFE. Unfortunately, many practitioners and academics are not familiar with this document due to its very limited publicity (only the printed version is available through the library of the Japanese Geotechnical Society). Perhaps the more recent literature is described in the suggested procedures for soft ground characterization by Ladd and co-workers (e.g., [11, 37]).

Typical soil sampling process is composed of nine stages as follows: (i) drilling, (ii) sampler penetration or block trimming, (iii) sampler extraction or block retrieval, (iv) tube/block sealing, (v) tube/block transport, (vi) tube/block storage, (vii) soil extrusion (only tube specimens), (viii) sample preparation, and (ix) laboratory testing. This process is schematically shown in Fig. 1 where the stress path followed by a soil specimen subjected to tube sampling is depicted. As observed in Fig. 1, soil sampling reduces the in situ mean effective stress, $p'_{\text{in situ}}$, even if soil disturbance is 'avoided'. Unfortunately, every stage of the sampling process may induce some degree of

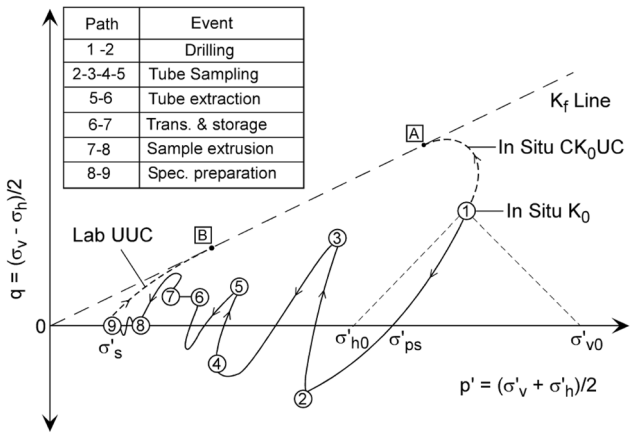

Fig. 1 Hypothetical stress path during tube sampling in low-OCR clay (from [37])

disturbance that changes further the stress state as well as the structure of natural soils. To what degree does each stage of sampling process contributes to the total disturbance in a given soil is, even nowadays, not easy to quantify. Soil disturbance is associated with [24]:

- Changes in the soil stress state.
- Mechanical deformation.
- Moisture content redistribution.
- Chemical reactions.
- Mixing and segregation of soil constituents.

A reduction in p' causes a decrease in yield stress, undrained shear strength, and soil compressibility. Therefore, proper engineering judgment is required to select sampling techniques that fit the soil conditions aimed at reducing the uncertainty associated with soil parameters obtained from laboratory tests. It is important to remark that despite its global nature, the answer to the sampling problem is local, because it needs to be grounded in local practice of drilling and sounding and be adapted to suit the local geological and geochemical conditions.

Sampling techniques are more or less effective in obtaining high-quality undisturbed samples depending on specific classes of soils, granular soils, by one side, and fine/clayey soils, by the other, or, in another level, the residual soils with weak relic interparticle structures. These techniques have been more recently consolidated, mostly due to some generalization of low-energy vibrational shear and compression wave (mostly seismic type) propagation velocities in lab specimens, which when conveniently normalized to in situ stress states can be compared with their values in natural conditions. Here the velocities are measured by geophysical techniques, now well recognized as valuable in ground investigation, even out of the scope of geotechnical earthquake analyses.

A laboratory-based characterization of soil behavior is directly dependent on the samples selected for testing and, therefore, dependent on their representativeness and quality in relation to the in situ conditions. The industrial investment in new high-performance samplers has been significant, proving its importance, not only for granular soils—silty, sandy, and gravelly materials—where the preservation of the natural structure is challenging, but also for clayey soils which are quite sensitive to the sampling operations. Recent studies [22] demonstrated that high-quality sampling, preservation, and specimen preparation are altogether primary key factors affecting reliable stiffness measurements even on stiff clays at small strains.

In granular soils, Gel-Push sampling (GP-S) has been adopted as an economical approach to obtain high-quality undisturbed samples without resorting to expensive ground freezing. The technology has been developed over the last decade in Japan [33], and also trialed in Taiwan [26] and

more recently, since 2013, introduced at KGHM Zelazny Most (ZM) copper tailings disposal located in southwest Poland, as described by Jamiolkowski and Masella [32]. Last year Dr. Kenji Mori, from Japan, one of the persons responsible for its development has presented a comprehensive keynote address in the ISSMGE-Technical Committee on Ground Characterization from In Situ Tests (TC102), fifth international conference held in Gold Coast, Australia, and its written document [48] will be herein partially transcripted.

After the M_w 6.2 earthquake of February 22, 2011 that struck beneath the city of Christchurch, New Zealand, a large research project was led by the University of Canterbury to characterize the engineering behavior of the soils in the region comprising in situ tests (cone penetration test, CPT, borehole drilling, and shear wave velocity profiling) and Gel-Push sampling followed by a program of laboratory testing including monotonic and cyclic testing of the soils [10]. This still on-going work has made use of the Gel-Push piston sampler at two trial locations in the CBD with great success [72], using a 70-mm-internal diameter Osterberg-type fixed-piston sampler (Osterberg 1979), modified for use with the polymer gel. More recently researchers from the same group [46] have shown that high-quality test specimens could be obtained using an Osterberg-type hydraulic fixed piston thin-walled sampler (the one that they have used was the Dames and Moore, DM, sampler) for predominantly silty and silty sand soils. This sampler uses a constant inner diameter, smooth brass tube with a relatively low area ratio of 7.6%. These features of the sampling tube coupled with the relatively short advancement length (45 cm) provided a means for retrieving high-quality samples of silty soils and medium dense sands. As referred in the work [46], shear wave velocity (V_s) determined on select number of specimens allowed to compare V_s-Lab and V_s-Field, with the results from these comparisons yielding reasonable trends with regard to V_s-Lab/V_s-Field ratios, as for the densities (void ratios) determined in the lab specimens and in those derived from correlations with in situ test results. The results in very loose and loose, relatively clean sands (SP and SP-SM) were the exception. In this case, the test results indicated that the sampling and testing procedures densified these soils.

Recently, [56, 57] presented the development of an innovative direct-push sampler specifically designed to reduce sample disturbance and maximize sample retention. The sampler performance for testing soft clays was proved by laboratory tests, including computer axial tomography (CAT) scans to evaluate the reliability of the sampler and also to estimate sample disturbance. It is very important to be able to assess the quality of the samples, to guarantee that only high-quality samples are used for extensive laboratory characterization. Different methods for the assessment of sampling quality have been proposed over the years relying on: fabric inspection; measurement of initial mean effective stress, p' [37]; measurement of strains during reconsolidation [43]; and comparison of in situ and laboratory measurements of seismic wave velocities [21, 38, 49, 64, 68]. It is worth highlighting that among the commonly used methods for assessing sample quality, the last is the only one capable of effectively considering the effects of destructuration in soils with low reconsolidation strains and conditions ahead of the advancing borehole during drilling operations; penetration of the sampling tube and sample retrieval to ground surface; water content redistribution in the tube; extrusion of the sample from the tube; drying and/or changes in water pressures; stress relief due to the removal of the sample from the ground to zero total stress state in the laboratory; and trimming and other processes required to prepare specimens for laboratory testing [80].

The effects of laboratory specimen preparation have also been investigated by measuring seismic wave velocities in high-quality block samples before and after trimming cylindrical specimens [7]. An average drop of 10% in shear wave velocity was measured in the cylindrical specimens, compared to that measured in the original block sample, evidencing minimal disturbance. However, the last tested specimens, over 2 months after trimming from the block, showed a 30% reduction of shear wave velocity, indicating that aging during storage is an influential parameter in the shear stiffness of a soil, as also pointed out by [19].

Sampling in sand-like soils and representativeness of in situ state conditions

Natural soils with highly sensitive structural features

Residual soils: focus on stress–strain response, from the very small stiffness

Residual soils are abundant in many parts of the world. These geomaterials result from in situ weathering of igneous, sedimentary, and metamorphic rocks. The degree and extent of weathering varies considerably with depth, hence weathered rock profiles may contain material grades from fresh rock to completely weathered material, usually classified as residual soil. When sampling these profiles, it is, therefore, inevitable to penetrate through several different grades of geomaterials. Due to their specific genesis, these soils present complex characteristics, which are a consequence of the overall variability and heterogeneity of the parent rock, as well as of the spatial arrangement and

distribution of the particles and pore spaces. The resulting residual soil is characterized by the presence of a bonded structure and fabric, which has significant influence on its engineering behavior, particularly in its small-strain stiffness properties [75]. Sampling problems are due to the difficulty in preserving its relict structure and its partial saturation, as well as the variability of the soil fabric, namely the presence of hard weathered rock fragments in a soft soil matrix. For these reasons, conventional tube sampling is expected to introduce some degree of disturbance, and only block sampling can be reliably considered undisturbed. Results obtained by Ferreira et al. [21] on two experimental sites on Porto residual soil enabled to identify considerable differences in the sampling quality of block and tube samples recovered by different samplers (e.g., driven samplers with various cutting edges, Mazier, Osterberg, Shelby) by the comparison of in situ and laboratory shear wave velocities. When these studies were developed Gel-Push samplers were not available, but recently [84] have presented excellent results in residual soils from Jurong formation in the western part of Singapore.

The experimental sites were selected where the natural variability of soil characteristics was considered to be acceptable for the objectives of this research. Extensive geotechnical in situ and laboratory characterization was carried out for each site, and many results and discussions have already been published [78] and more thoroughly analyzed and compared with other residual soils in [19, 76].

The first experimental site (ES1) was located in the region of Porto, where extensive geotechnical in situ and laboratory characterization had already been carried out (e.g., [75]). This site presents a typical saprolitic residual soil, resulting from the weathering of Porto granite, and it is essentially composed of alkaline granite, coarse to medium grains, two mica, and albite as main feldspar. The second experimental site (ES2) is located within the campus of the Faculty of Engineering of the University of Porto (FEUP) and was initially used for an international pile prediction event, under the scope of ISC'2 (International Conference on Site Characterisation) held in Porto in 2004 [78]. Essentially, the site is geologically formed by an upper layer of heterogeneous saprolitic residual soil from granite of variable thickness, overlaying a weathered granite, in contact with high-grade metamorphic rocks (gneisses and migmatites). The sampling processes used for retrieving soil specimens from the experimental sites can be divided into three types, according to the sampling methods which are directly related to the quality of the obtained samples: (a) block samples; (b) "undisturbed" tube samples; and (c) disturbed soil samples. A soil sample is considered intact or undisturbed when the soil structure and mechanical properties are kept as close as possible to those of the soil in the field.

There are a number of undisturbed tube sampling techniques currently in use in Portugal, usually divided into driven samplers and rotary samplers. A few of these techniques were selected for borehole sampling in ES1. The experimental site ES1 served as ground for the assessment of the sampling quality of a variety of tools and techniques, with the purpose of selecting the most suited sampler for this soil to be used in ES2.

For obtaining the highest quality samples, as undisturbed as possible, a number of block samples were collected at both experimental sites. The block sampling process can be divided essentially into the following four stages (JGS 1995): (i) rough carving of the sample, by opening of the area surrounding the intended sample; (ii) trimming of the sample, performed with great care, to obtain the intended sample size, well aligned for a perfect fit in the container; (iii) sealing of the sample, by the insertion of the container covered with plastic film for moisture retention; (iv) separation from the ground, by cutting the block on the bottom. Finally, the block is slowly and carefully tilted to reveal the bottom surface, which is immediately leveled, sealed, and covered with the box cover [21]. Photographs of the work at ES1, where three cubical blocks of circa 400 mm were retrieved at a depth of 2 m, are presented in Fig. 2, to illustrate each corresponding sampling stage. At experimental site ES2, six block samples were collected, two at each of the depths of 1.65, 2.75, and 4.25 m.

As described by Ferreira et al. [21], the tube sampling surveys were performed in collaboration with private engineering contractors, which were responsible for boring and extracting soil samples using the available samplers, according to their own standard procedures. The selection of the samplers used in the sites was made considering a few fundamental aspects, namely (a) the characteristics of this soil; (b) some variety of geometric properties of the samplers, such as cutting edge, sampler driving method, existence or not of inside clearance, the use of liner and its type; (c) availability of equipment; (d) level of applicability in practice; (e) expected sample quality offered by the different samplers. At ES1, six sampling boreholes were selected to form a triangular arrangement, with an even spacing of 4 m, to facilitate seismic cross-hole testing. A different sampler was used in each borehole and soil samples were collected at the depths of 2, 4, and 6 m. A list of the samplers used, including rotary and driven samplers with standard and sharp cutting edges, and a summary of characteristics are presented in Table 1 and a view of the samplers is illustrated in Fig. 3.

The GMPV sampler is a thick-walled sampler, manufactured by the Spanish company TECSO®, of about

Fig. 2 Illustration of block sampling stages in residual soils the work at experimental site ES1 in Porto (adapted from [21])

Table 1 Tube sampler used in each borehole at ES1

#	Sampler	Cutting edge (°)	Internal diameter (mm)	Liner	Sampling
S1	GMPV	30	72.0	Gray PVC	Dynamic
S2	ST85	5–6	75.0	PVC (often transparent)	Dynamic
S3	NT81	5–7	74.0	Coated steel (not stainless)	Dynamic
S4	Mazier	[a]	74.0	Blue PVC	Rotary
S5	Osterberg	30	n/a	None	Stationary
S6	Shelby	30	77.5	None	Stationary

[a] Sharp cutting edge ahead of the drill bit

(a) S1 **(b)** S2 **(c)** S3 **(d)** S4 **(e)** S6

Fig. 3 Pictures of the different samplers used in the experimental site ES1

600 mm of length, external diameter of 90 mm and internal diameter of 72 mm, and a cutting edge of 30°. In Fig. 6 are presented photographs taken during the sampling process, together with a schematic diagram of the sampler.

The ST85 is also a thick-walled sampler and is manufactured by TECSO®. It has 600 mm of length, an internal diameter of 75 mm, and an internal transparent PVC liner (Fig. 9). The particularity of this sampler resides in its cutting shoe, which has a sharp cutting edge of 5°–6°. This detail, in contrast with the traditional cutting shoe angles (of 30°–40°), represents an important quality leap towards undisturbed high-quality tube samples [19].

The NT81 sampler was developed more recently by TECSO®, based on the design of the ST85, just presented. The design changes imposed an area ratio lower than 25, for thick-walled samplers. For this purpose, the ST85 suffered minor modifications, which are mainly related to the change of liner material. In the NT81, the liner is thinner and made of steel. To ease extraction after sampling, this liner is pre-cut longitudinally. The obtained sample diameter is 74 mm. Figure 4 shows a simplified scheme of this sampler and its application during the sampling stage.

Mazier sampler, manufactured by the French company Seditech, is considered in the industry, as particularly interesting for sampling, due to its dual capability of static boring, in an analogy with the Laval sampler development [39], and its flexibility in driving in harder soils. This sampler consists of a rotary triple tube, with a low wall coefficient, containing a polyethylene liner. The available internal diameters range from 61 to 108.5 mm. In this sampling program, a sampler with an internal diameter of 74 mm was used. Long samples can be retrieved, of about 1000 mm. A diagram of the operation of this sampler in different soil conditions is presented together with the sampling process and schematic in Fig. 5.

The Osterberg sampler is a thin-walled stationary sampler designed to sample soft soils. Nevertheless, its application was considered has been enlarged for other materials, which proved unsuccessful in some cases, like residual soils due to its coarse-grained nature, while other had performed well (this will be discussed below for loose

Fig. 4 NT 81 sampler: **a** schematic diagram; **b** photographs of the steel liner and of the sampler during sampling stage at the CICCOPN experimental site

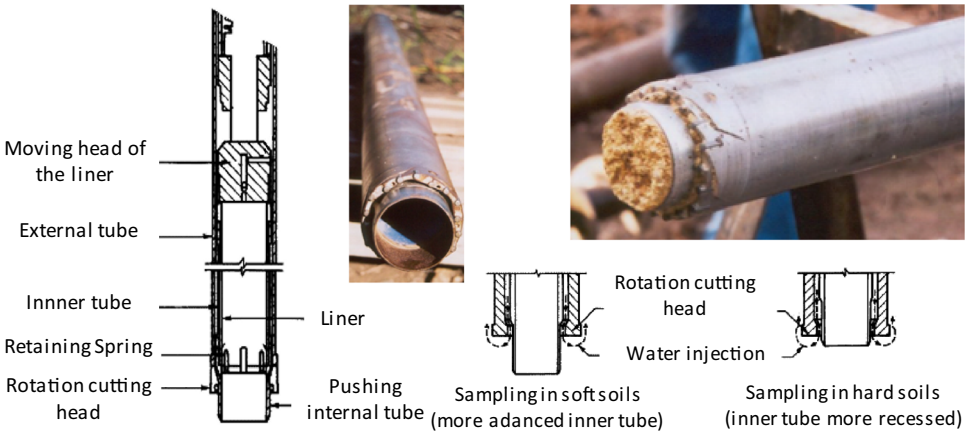

Fig. 5 Mazier operation and process: diagram, scheme, and illustration on field

to medium silty sands). The sampler shows some inaptitude to operate in coarse granular geomaterials. The Shelby sampler is a thin-walled sampler commonly used in Portugal. The collection tubes are made of steel, seamless with no inside clearance, with 500 mm length, 77.5 mm internal diameter and about 3 mm wall thickness. The cutting edge angle is of 30°. The tube insulation system comprises a rubber lid, slightly wider than the tube at the base, and a double steel tip with an O-ring at the top and a lower diameter than the internal diameter of the sampler, to ensure a good fit with the top end of the sample. Figure 6 illustrates these two "classical" samplers.

Since Shelby is also a stationary sampler, it is best suited for sampling materials with no or few coarse elements, and consequently it is less suitable for sampling residual soils. Using higher diameters may be an interesting option, but due to the smoothness of the inner walls of the sampler, sample collection may be compromised by the risk of fall of the sample. For the removal of the sample from the tube and considering its length and material (steel), it is necessary to use an extractor. This piece of equipment compresses the soil sample on one side of the sampling tube, pushing the sample out until it slides along the tube. This procedure involves some degree of disturbance to the samples, especially for the case of lightly bonded and structured materials, such as these residual soils [19].

The results obtained for the testing program were analyzed for sampling quality assessment by the measurement of strains during reconsolidation [43]. This method was applied to a number of ES1 samples, from various tube and block samples, where a greater variety of tube samplers were used. Despite the clear differences between the various samples collected in ES1, the values of $\Delta e/e_0$ obtained in this exercise were all below the minimum proposed value of 0.04 (as interpreted from [43]) except for one of the reconstituted samples, which were included as an indication of the poorest quality sample (in which the original soil structure has been completely lost). It can be concluded that this method alone is not appropriate for assessing the sampling quality on this soil, since it would classify all samples as very good to excellent quality samples. Clearly, the relatively low compressibility of this

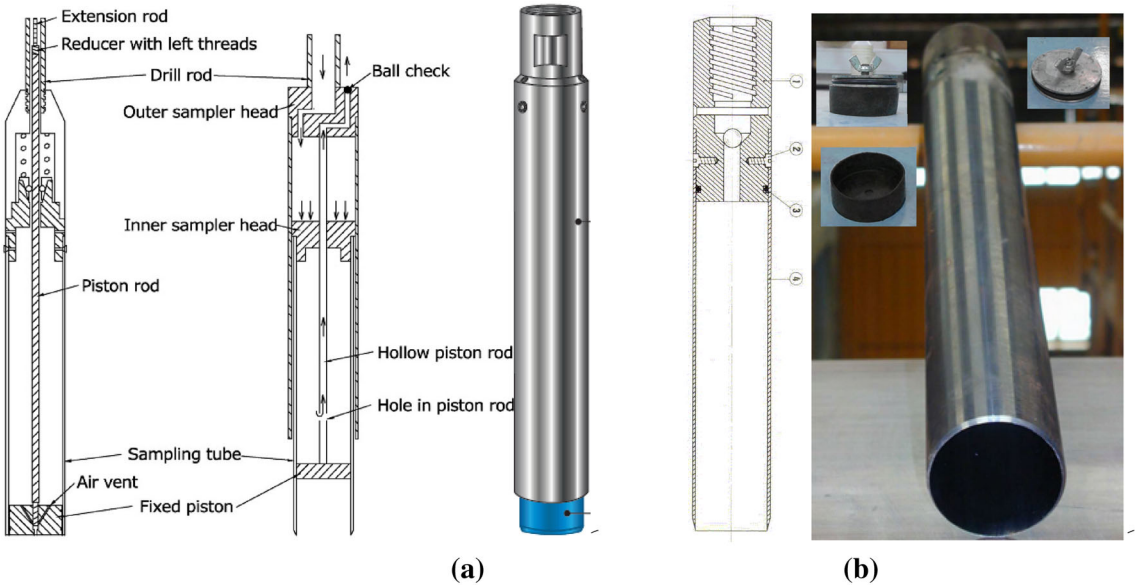

Fig. 6 Osterberg composite hydraulic fixed piston (**a**) and Shelby stationary (**b**) samplers: schematic photographs of the sampler and the insulating lids

soil compromises the direct application of this method. To establish a more suitable sample quality classification, different limits or scale ranges for each category would have to be defined for this type of soils. This method is, however, considered useful for a qualitative and comparative analysis of the tested samples.

Assessment of sampling quality by comparison of seismic wave velocities

For the measurement of shear wave velocities in the laboratory, bender elements (BE) were mounted in the top and bottom platens of triaxial chambers. These transducers are a powerful and increasingly common laboratory tool for determining the shear wave velocity, V_S, and hence the small strain shear modulus, G_0, in geomaterials. There are several advantages of BE testing, namely its simplicity and ease of use, but there is still no standard developed for the testing procedures or for the interpretation of the results. This often leads to a high degree of uncertainty and subjectivity in the interpretation. In this research, the framework for BE testing and interpretation proposed by Viana [79] was applied.

The loss of shear wave velocity from in situ to the laboratory ranged between 14% (block samples) to nearly 50% for some of the tube samples. Ng and Wang [50], Ng et al. [52], and Ng and Leung [51] also measured shear wave velocities on block specimens of completely decomposed granite and tuff, reporting values around 30% higher than those of the Mazier specimens. More recently, Rocchi and Coop [60] reported small disturbance on Mazier-collected specimens on Hong Kong residual soil, which may be a result of the grading characteristics of the soil and to a higher weathering degree.

According to Ferreira et al. [21], for residual soils, considering the stages of a sample (from sampling, to storage, preparation, and finally to laboratory testing) shear velocity losses below 15% appear to be minimal and, therefore, acceptable as an indicator of an excellent quality sample. A gradual scale can then be empirically and experimentally established: below 30% for a very good quality sample; below 40% for a good sample; below 50% for a fair quality sample. For a loss in V_S above 50%, the quality of the sample is poor and the sample should be considered disturbed; therefore, unsuitable for careful laboratory testing and characterization.

For the comparison between laboratory and in situ measurements of seismic wave velocities, the results obtained for the tested specimens of both experimental sites were analyzed at the estimated in situ stresses. For a more consistent comparison, the shear wave velocities were normalized to the respective void ratio. The need for normalization to the void ratio derives from the observation of significant differences among the initial void ratios of the various tube samples and the block and in situ conditions (details in [19, 21]). The tube sampling process tends to compress the samples, inducing some degree of disturbance. Since the shear modulus is strongly dependent on the void ratio, this normalization enables to clearly capture sampling disturbance, since it comprises not only destructuration but also volume change of the soil sample. For example, the sample with the lowest void ratio (more

severely compressed) exhibits a higher shear modulus than the in situ data, despite its destructuration; after normalization, this sample has the lowest normalized modulus.

It was assumed that the block sampling process did not induce any measurable changes in the compaction conditions of the soil, that is, the void ratio of the block samples was assumed identical to that of the soil at natural in situ conditions, at the corresponding depths. Therefore, in situ seismic cross-hole (CH) and down-hole (DH) tests were executed to determine wave velocity results. The results were normalized, considering the void ratio of the block samples, according to the function proposed by Lo Presti [42] which provided the best match with the evolution of the shear modulus at unload–reload cycles of a reconstituted specimen, defined as follows:

$$V_S = \sqrt{\frac{G}{\rho}} = C \cdot \sqrt{F(e)} \cdot \sigma_v'^{n_a} \cdot \sigma_h'^{n_b} \quad (1)$$

$$F(e) = e^{-1.3} \quad (2)$$

Therefore, the measured shear wave velocities were normalized as follows:

$$V_S* = \frac{V_S}{\sqrt{F(e)}} \quad (3)$$

A summary of the normalized results is presented in Fig. 7a, b for ES1 and ES2, respectively. For the ES1 samples, shown in Fig. 7, only V_{Svh} were measured. The differences between V_{Shv} (from cross-hole tests) and V_{Svh} (from down-hole) were found to be small and, in the context of this study, these will not be distinguished. Laboratory samples were nor The similarity of V_S trends in depth from both in situ and laboratory tests is evident for both experimental sites and the differences encountered can be mainly attributed to disturbances associated with the sampling processes.

In terms of the tube samples (S1–S6) collected at ES1, the results show that the geometric characteristics of the sampler, both in terms of the cutting edge angle as well as of the area ratio were decisive. The sampler with the lowest outside cutting edge angle (S3) provided the highest stiffnesses. The good performance of the Shelby sampler (S6) is worth mentioning, which is most likely associated with the difference between the internal diameter of the sampling tube and the final diameter of the tested specimens, requiring the trimming of the sample to the appropriate size, after its extrusion from the sampler. This process, despite being quite delicate, removal of the peripheral areas of the sample that had experienced greater distortions during both sampling and extrusion, highlighting the relevance of careful laboratory sample preparation techniques and, whenever possible, the use of large diameter samplers. Finally, samples collected by the Mazier sampler are unexpectedly damaged. Its disturbance is probably related to the operational requirement of applying high water injection pressures at the cutting shoe to reduce the friction and abrasion between the cutting tools and the coarse quartz grains of the soil. The injected water literally washed away the fragile bonds between the particles, severely damaging the natural structure of the soil.

For experimental site ES2, as previously mentioned, only one tube sampler was used for collecting all the samples: the same tube sampler used for borehole S3 in ES1, that is, NT81. This tube sampler was selected for its good performance in terms of sampling quality of the residual soil from ES1. In this case, a fewer number of samples were tested at the estimated in situ stresses, as presented in Fig. 7b. The figure shows that the differences

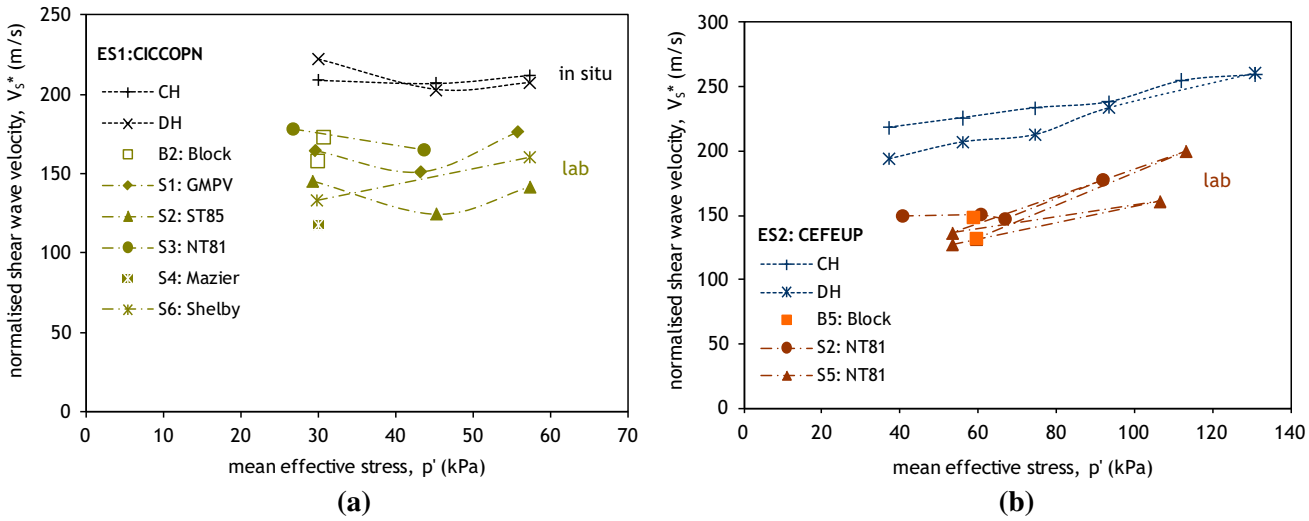

Fig. 7 Normalized shear wave velocities for: **a** ES1 specimens, and **b** ES2 specimens (adapted from [21])

between the shear wave velocities of different samples are smaller than those observed for the samples of ES1. This was anticipated since all samples were collected by the same sampler. The evolution of the laboratory and in situ velocities with stress, that is, with depth, is relatively similar, and it is unclear whether sample disturbance is affected (or not) by the depth of sampling. Contrary to the results for ES1 samples, in this case, the block samples appear to have the same loss in shear wave velocity in relation to the in situ value as the tube samples. This would mean that those blocks have the same level of disturbance, which is unlikely. A more plausible explanation for the unexpectedly lower values of the block sample results may reside on the fact that the two block samples were tested much later than the tube samples. Aging during storage is an influential parameter in the shear stiffness of a soil, which, however, was not explicitly and systematically addressed in the context of this research. The effects of laboratory specimen preparation on changes in natural residual soil specimens have also been investigated by measuring seismic wave velocities in high-quality block samples before and after trimming cylindrical specimens [7]. An average drop of 10% in shear wave velocity was measured in the cylindrical specimens, compared to that measured in the original block sample, evidencing minimal disturbance. However, the last tested specimens, over 2 months after trimming from the block, showed a 30% reduction of shear wave velocity, indicating that aging during storage is an influential parameter in the shear stiffness of a soil, as also pointed out by Ferreira [19].

The results from both experimental sites have been combined by plotting the normalized laboratory V_S values against the corresponding normalized in situ values (for the same depth, or mean effective stress), as shown in Fig. 8. Perfect agreement of laboratory and field results would fall on the 1:1 line; below this line, the points indicate that laboratory values are lower than in situ values.

It is worth noting the position of the reconstituted sample, located at quality zone D, therefore, not corresponding to the lowest shear wave velocity value. Two tube samples (from S2 and S4) appear below the reconstituted sample, which is indicative of their poor quality, thus enabling to confirm the proposed limits of this classification. There is some parallelism between this new classification and that proposed by [38] based upon tests on Boston blue clay and [68] for Bothkennar soft clay. In their research, these authors compared laboratory and in situ shear wave velocities and used the reconsolidation strains method by Lunne et al. [43] to define the categories of sample quality. Other authors applied this methodology to soft clays [15]. However, their classification is less restrictive than the one proposed by Ferreira et al. [21]: the ratio $V_{lab}/V_{in\ situ}$ from 0.6 to 0.8 corresponded to good-to-excellent-quality samples; poor-quality samples had a ratio of 0.35–0.6 and very poor-quality samples exhibit values of $V_{lab}/V_{in\ situ}$ lower than 0.35.

More recently, Rocchi and Coop [60] have presented a new approach to saprolites and residual soils that have wide ranges of particle size distribution, mineralogy or particle morphology. The particle arrangement or possible bonds between them (soil structure) evolve with weathering [74, 75, 77, 78], which demanded for studying changes in the physical and mechanical properties of a saprolite along a profile ranging from highly decomposed granite (HDG) to completely decomposed granite (CDG), belonging to grades IV and V according to Geotechnical Engineering Office classification system (GEO 1988). As described by the authors, a series of one-dimensional compression and triaxial tests was carried out. Both the reconstituted and intact specimens recoiled with a Mazier

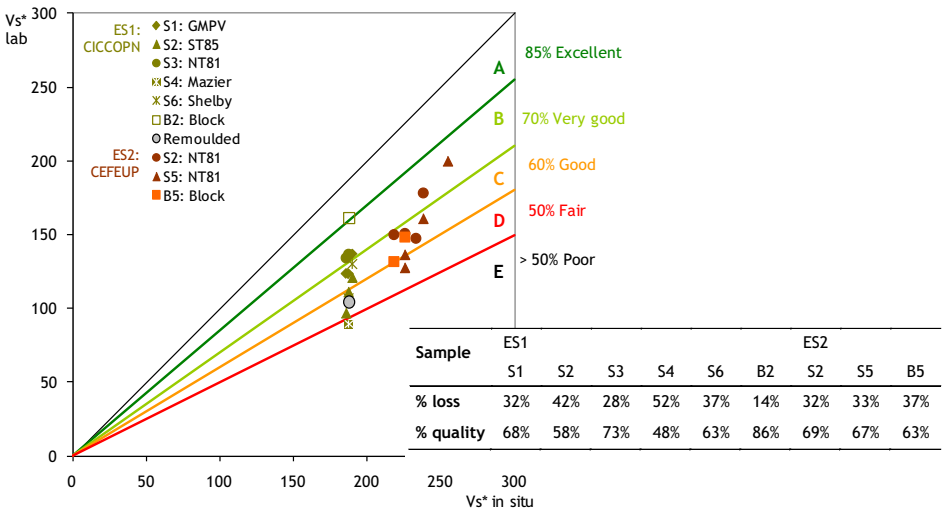

Sample	ES1						ES2		
	S1	S2	S3	S4	S6	B2	S2	S5	B5
% loss	32%	42%	28%	52%	37%	14%	32%	33%	37%
% quality	68%	58%	73%	48%	63%	86%	69%	67%	63%

Fig. 8 Proposed classification of sampling quality based on the comparison of normalized shear wave velocities in the field and in the laboratory (single-column width), (adapted from [21])

sampling system were similar in size, with these latest Mazier intact samples taken from an adjacent core. In the reconstituted specimens, a unique mean particle size distribution was imposed for each degree of weathering to facilitate establishing the intrinsic properties. Results were interpreted within the critical state framework.

The preparation of the intact samples was described as follows [60]: generally, the intact Mazier samples for triaxial testing were cut to the required length with a diamond saw while still in the plastic lining. The plastic tube was then very carefully removed, cutting several longitudinal slots along it using an end cutter in a purpose-built rig that supported the sample throughout the process, therefore, minimizing disturbance. The perimeter of the sample was not trimmed further, even if the external part would be disturbed by the coring process. This was because when the perimeter was trimmed, there were severe problems due to membrane puncture caused by protruding particles. Despite the presence of the disturbed circumference, as will be discussed later, the volume changes of the whole sample did not indicate that the overall sample disturbance was particularly severe. A few initial samples (of HDG and vwCDG) were first removed from the casing and then trimmed manually to the required length. Owing to the difficulties encountered, a small amount of plaster had to be used to ensure even and planar faces, similar to the oedometer tests. The sample disturbance effects were in this case confirmed not to be large, based on a criterion obtained from a test on a block sample. Small disturbance was achieved developing new techniques to trim and test the intact specimens and the results obtained suggest that Mazier samples might be of suitable quality for measuring the effects of structure, provided that the plastic lining is removed avoiding extrusion. When comparing stiffness values for the Mazier and block samples, similar values were found and the differences between the intact and reconstituted specimens were also comparable. There was no real evidence of any trend with weathering for the stiffnesses of the intact soils, but there were significant effects of structure that increased the stiffness of the intact soil with respect to the reconstituted.

This work highlights the need for good quality samples. When considering large strain behavior the effects of the structure were reduced as weathering proceeded, although this was clearer when analyzing the behavior in shear than in compression. Reducing effects of structure with weathering might also be expected for other weathered soils but require testing of both reconstituted and good quality intact samples to be quantified. The in situ values of the state parameter, which depends both on the in situ state and the location of the CSL* that changes with weathering, were always below the CSL* and its values increased with weathering, similar to the specific volume.

Natural sands and non-plastic silty sands: focus on cyclic instability—earthquake engineering

Tube sampling in sands is drained, so volumetric as well as shear strains will occur. It is highly probable that the magnitude of the shear strains will be sufficient to destructure the sand, particularly since yield strains in granular materials are low. The volumetric shear strains caused by sampling will depend on the initial density of the sand being sampled: initially loose sand will contract and densify, while initially dense sand will dilate and reduce in density [45].

Truly undisturbed samples of sand can only be obtained if the in situ sand structure is preserved before sampling. Clean sands have been shown to be particularly difficult to sample due to volume changes during sampling resulting in compression or dilation of the sample caused by the high friction mobilized between sample and internal tube walls, or soil relaxation allowed to occur within a tube with larger diameter than the cut sample; retrieval and associated changes in effective stress, which in turn result in deformation of the sample; transportation and preparation for testing in the laboratory (vibration under low effective stress) requiring special care to avoid additional gross disturbance of the soil sample and/or collapse [66]. Singh et al. [65] demonstrated that the characteristics of sandy soils (including in situ stresses) could be effectively preserved by freezing the ground. Samples are frozen in situ before being retrieved by coring through the frozen soil mass, and/or retrieving using a crane. These issues favored the development of the freeze sampling technique, where samples are frozen in situ before being retrieved by coring through the frozen soil mass, and/or retrieving using a crane. Despite being an excellent technique for obtaining undisturbed samples, the freezing process is complex and expensive, and only justifiable in specific, high-level projects. This method is, however, limited to shallow depths, besides introducing volumetric changes in the water surrounding soil particles. Moreover, ground freezing may cause drifting of fines content in silty sands and disturbance on the sensitive microstructure of these soils would likely occur during freezing and thawing process. The difficulty in obtaining undisturbed samples in saturated clean to silty sands, namely due to the excessive friction generated during penetration of conventional tube samplers, is known to cause serious disturbance to the specimens. As a result, subsequent advanced laboratory characterization would be severely compromised, particularly for studies involving cyclic instability and the assessment of liquefaction potential. Recently, the "Gel-Push" sampling technique has been developed and successfully employed to obtain undisturbed samples on non-plastic silty sands, namely in liquefaction sites in southern Taiwan, Christchurch in New

Zealand, or Tokyo Bay in Japan [26, 40], as well as in very difficult non-plastic tailings in Zelazny Most in Poland [32].

As described in ISC'5 keynote lectures by Mori and Sakai [48], the new type of sampler called the GP sampler was designed to sample gravelly soils, but has proven to be successful in sampling soils ranging from dense sand, to gravel, as well as sedimentary rocks. The sampler is constructed by a single-core barrel and uses a viscous polymer gel as its drilling fluid. The polymer plays a key role in obtaining high-quality samples, helping to preserve the soil structure. The polymer gel was also employed in more traditional style samplers, in an effort to improve the quality of samples obtained from silt, silty sand, and sand. These attempts have experienced difficulties or failed, while the GP samplers have been successful, making a qualitative difference in the sampling of granular soils for engineering purposes. Following the description of that keynote address, the four variations of GP samplers, each specifically useful for a particular sampling requirement: GP-Rotary, GP-Drilling, GP-Triple, and GP-Static, referred by the authors as GP-R, GP-D, GP-Tr, and GP-S in the rest of their text [48]. In that document, a table summarizes the principal features of each one of the GP samplers, which they summarize as follows (quoting):

- The GP-R sampler is a single-core barrel sampler designed to obtain high-quality samples of sands, gravels and sedimentary rocks, having a high flexibility in accommodating a wide range of formations;
- the GP-R sampler was designed for sampling at the ground surface, or from an excavated trench;
- the GP-D sampler was developed to conduct equally high-quality sampling in boreholes. It has the same basic construction as the GP-R, but is fitted with a special "catcher" mechanism that enables it to retain the core inside the sampler during retraction from the ground and borehole;
- the GP-Tr and GP-S samplers were designed around a rotary triple tube sampler and the Osterberg sampler, respectively. They both use the highly viscous polymer solution to reduce friction between the cored sample and sampler tube wall, minimizing one of the primary causes of sample disturbance.

In the referred document [48], the authors describe thoroughly the different versions of GP samplers and give emphasis to the polymer used in this process, as it vital role in GP sampling. As it is remarked, the basic polymer is a partially hydrolyzed polyacrylamide and is commonly called PHP polymer. Although available around the world, viscosity characteristics vary depending on the manufacturer, with the product locally available in Japan eventually distinct from PHP polymers produced elsewhere. The polymer is sold in liquid form dissolved in mineral oil. In this paper, the authors present a series of specific properties of the solution, emphasizing that, for a particular high concentration solution of 2.5:4% ratio of polymer to water, possible with the product available in Japan, a fluid whose viscosity is more than ten times thicker than the industry norm of 0.1:0.4% is created (details in [83]. This polymer solution is very thick and viscous when it is still, but becomes more fluid like when it is sheared. This behavior is known as "shear thinning". During the sampling process, the barrel rotates at high values of rpm depending on the size of the barrel. The polymer solution flowing alongside the barrel wall in the annular space is sheared by the high rotational speed and loses viscosity. This zone of low-viscosity polymer solution acts like a protective membrane, isolating the cored sample from the barrel's rotational motion. Stringer et al. [66, 67] report that GP sampling is currently carried out in Christchurch with one of three types of samplers: GP-S, GP-TR and GP-D, with the key and common feature of the samplers being the delivery of a lubricating polymer gel to the bottom end of the samplers. Figure 9 shows an example (from sampling) of the gel coating the bottom end of the sample using the GP-S sampler. The gel coats the sample, with the aim of significantly reducing the friction between the sample and core barrel. Once retrieved from the tool, the sample shown in that figure slid easily in and out of the tube with only minor slope angles from the horizontal.

As noted by Mori and Sakai [48], unlike conventional drilling fluid, which tends to wash out fine particles, the polymer solution's high viscosity and slow flow rate leave the fines undisturbed. Since the fines act as a matrix material, holding the coarser particles or gravels in place, sample disturbance during the polymer gel sampler coring is kept to a minimum. The sheared solution essentially seals the cored sample as it flows downward to exit the barrel at and around the bit, cooling the bit and carrying away the cuttings as it passes out of the barrel into the borehole (further details in the keynote paper).

Fig. 9 Lubricating polymer gel coating soil sample (from [66])

The GP-R and the GP-D samplers

The GP-R sampler was originally designed for sampling gravel formations at the ground surface, while the GP-D sampler is a single-core barrel sampler that has been specifically engineered to operate in boreholes. The former is a single-core barrel sampler, available in barrel diameters of 100, 150, 200, and 300 mm. Figure 10a depicts a GP-R sampler with the sample having entered about one-third of the way into the core barrel. As described tailed by Mori and Sakai [48] the sampler barrel is filled with the polymer solution and placed at the ground surface, wish, while is turned and pushed downward, an impregnated diamond bit cuts into the ground. This specific bit is smooth to touch and grinds through granular soils and other ground formations with minimum disturbance. The sample core, with its mortar cap, is forced into the barrel as the sample cuts it from the surrounding soil, pushing the stored polymer solution up, and squeezing it over and around the core into an annular space of about 1 mm between the core and the barrel wall. The GP-D sampler (in diameters of 100, 150, and 200 mm), represented in Fig. 10b has essentially the same construction as the GP-R, having added some features allow working inside boreholes in depth: the introduction of a free piston, a core lifter, and a polymer solution supply connection at the sampler head.

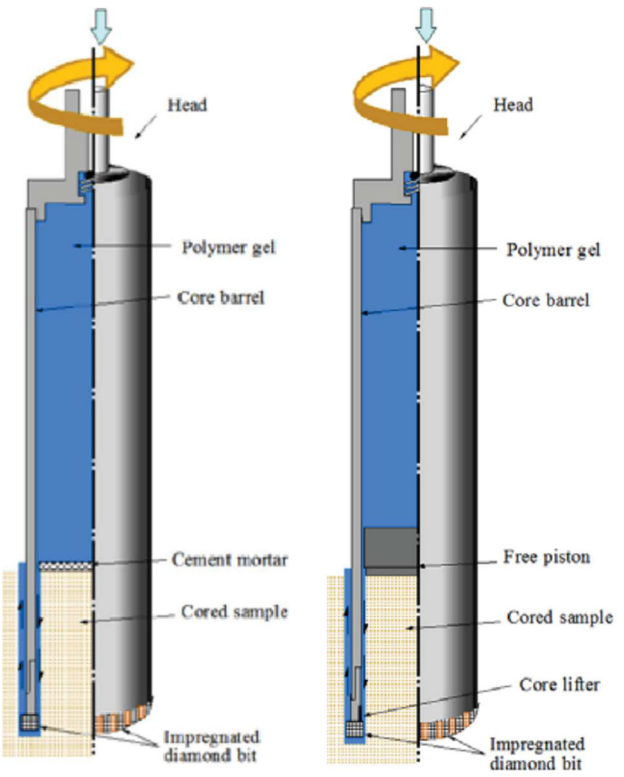

Fig. 10 **a** Cross section of GP-R sampler with cored sample entering into the sampler barrel; **b** cross section of GP-D sampler with cored sample entering into the sampler barrel (adapted form [48])

As emphasized by Mori and Sakai [48] one of the beneficial features of both the GP-R and GP-D samplers is their use of an electrically powered motor for coring. The motor can be preprogrammed to precisely control the sampler's rotational speed and penetration rate. In stark contrast to the oscillation caused by diesel motors, the electric motor produces very little vibration and consequently, significantly less disturbance to the sample and the subject soil. Following the authors' description, the free piston of the GP-D sampler serves as a plug at the bottom end of the barrel, and prevents the polymer solution from leaking out of the barrel while the sampler is being lowered down the borehole. Once the sampler is positioned on the bottom of the borehole, the barrel begins to rotate, cutting the sample. The free piston is pushed upwards by the entering core, forcing the polymer to flow into the annular space between the core and the barrel. Finally, it exits the barrel in the same way as in the GP-R sampling process, cooling the bit and carrying away the cuttings. Since a wedge cannot be driven in the borehole to separate the core from the ground, a core lifter is fitted just above the bit to squeeze the core sample, holding it in the barrel as the sampler is raised from the borehole. The lifter mechanism is a circular band (illustrated in the referred ISC'5 KN paper) and the when the coring is completed, the sampler barrel is nominally lifted, still attached to the formation site, the core sample resists the pull, slumping down slightly, and dragging the core lifter with it. This triggers the core lifter mechanism, causing it to tighten around the cored sample, and enabling the sample to break free from the ground. Finally, with the sample secured, the GP-D barrel is raised to the surface for sample extraction. The authors remark also that, since the GP-D sampler rotates at a very high speed, multiple centralizers are placed on the drill strings to ensure smooth, vibration-free coring.

The GP-TR and GP-S samplers

As described by Mori and Sakai [48], the GP-Tr sampler is designed for sampling medium to dense sandy soils. It can sample sand containing some gravel, but not gravelly soil. As with all GP samplers, the GP-Tr uses the polymer solution in a unique way: relying on it as a lubricant to reduce the friction between the sample and the sampler tube. Its construction is based upon a conventional rotary triple tube sampler (as it is the case of the Mazier sampler), retaining the triple tube's basic features, including self-adjusting shoe penetration, stationary liner and inner tubes and an outer tube, tipped with a bit, that is employed to

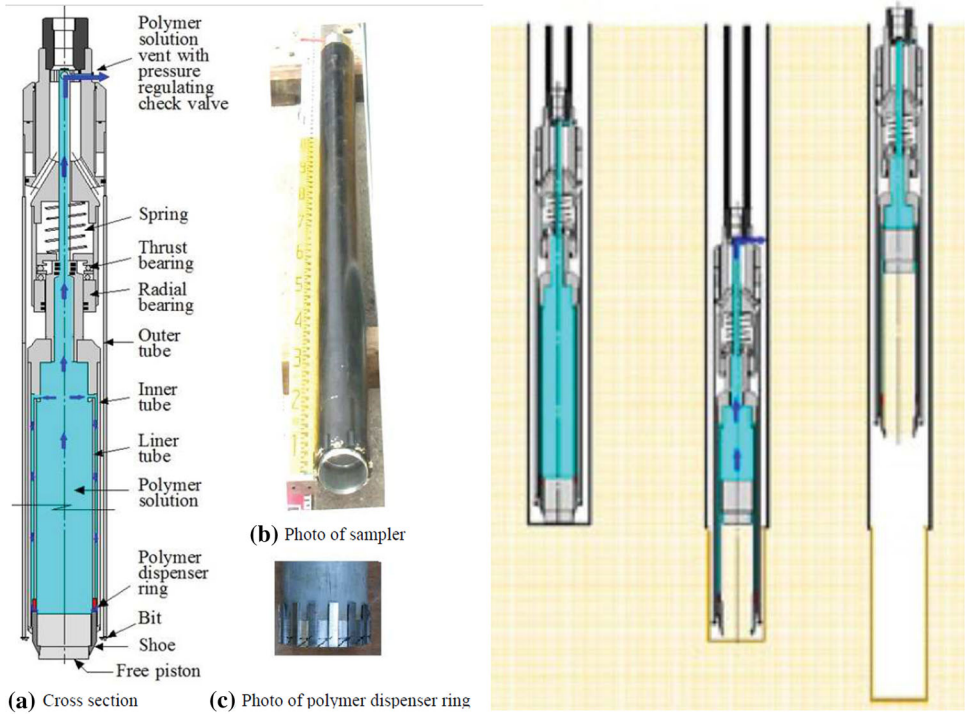

Fig. 11 Schematic illustration and photo of GP-Tr sampler (adapted from [48])

rotate and drill the soil above the shoe. Figure 11a–c shows schemes and pictures of the sampler. Unlike the GP-R and GP-D samplers, the GP-Tr utilizes ordinary drilling fluid to remove the cuttings and cool the bit; the ring is attached to the bottom end of the PVC liner tube. The GP-S sampler, developed as a joint project in 2006, between Kiso-Jiban Consultants and the Chinese Research Institute of Taiwan, led by Professor Lee, is fitted to obtain high-quality samples of silt, silty sand, and loose sand. Unlike the other GP samplers, it does not use the rotational motion of a drill bit to obtain a sample. Instead, the sampler tube penetrates the ground statically, having being designed from the Osterberg sampler, with a fixed piston, and using hydraulic pressure to push the sampler tube into the ground. The GP-S sampler has three pistons [48]: the stationary piston, the sampling tube-advancing piston, and the core catcher activating piston. The piston remains at the bottom of the borehole during the sampling. The sampling tube-advancing piston pushes the shoe, the sampling tube, and the liner into the ground simultaneously. It is remarked that there is a major modification to the conventional Osterberg model, which the fact that the GP-S sampler has a core catcher that is extended in position by a hydraulically activated piston. The core catcher acts to retain the cored sample, preventing it from falling out of the sample tube as it is retracted from the ground. The core catcher also dispenses a coating of thick polymer solution onto the surface of the cored sample, in a way similar to that of the dispenser ring in the GP-Tr sampler.

As illustrated by Stringer et al. [66]—Fig. 12—the GP-S samplers comprise three barrels, a fixed piston and a two traveling, having in the core-liner barrels a series of holes located near the top of the sample liner tube, which allows the outflow of polymer gel from the inner barrel during the sampling process. Similar layouts are presented by the authors for the GP-Tr sampler.

The methodology of GP-S sampler is as follows [66]: the sampler is lowered into the borehole to the depth of last rotary drilling, pushing the sampler past any slough which may have fallen into the hole; when it has reached the required sampling depth, the drill pipe is locked in place at the surface and the drill pipes are filled with water before being connected to a water pump. Before starting the pump, a bypass valve is opened so that flow is initially returned to the water reservoir. The bypass valve is gradually closed, so that pressure builds on the upper traveling piston. This pressure results in the middle barrel advancing the cutting shoe into the soil, while leaving the inner core barrel unstressed (Fig. 13); when the gel reaches the core catcher, it passes through the gaps between the catcher "fins" (scheme of the activation and photo of the core catcher in the same figure) and coats the surface of the soil sample as it enters the core barrel.

Quoting Stringer et al. [66], an O-ring seal on the outside of the fixed piston "wipes" the inside of the core barrel as it advances past the fixed piston, avoiding the gel to pass the fixed piston in either direction. During sampling, only a small fraction of the total gel placed within

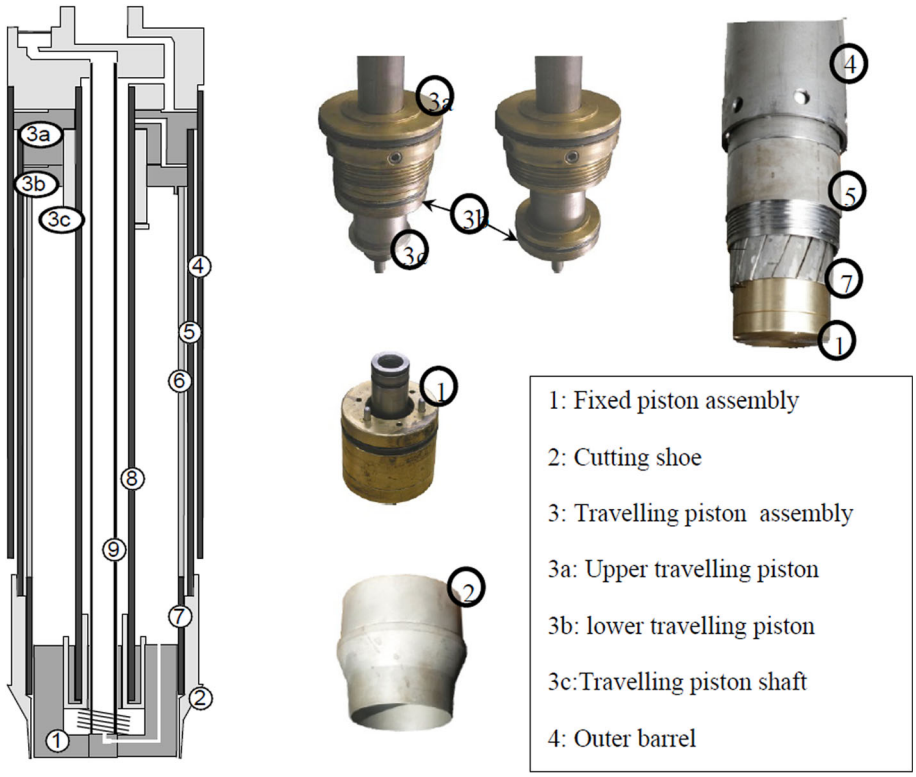

Fig. 12 GP-S sampler schematic and key components (adapted from [66])

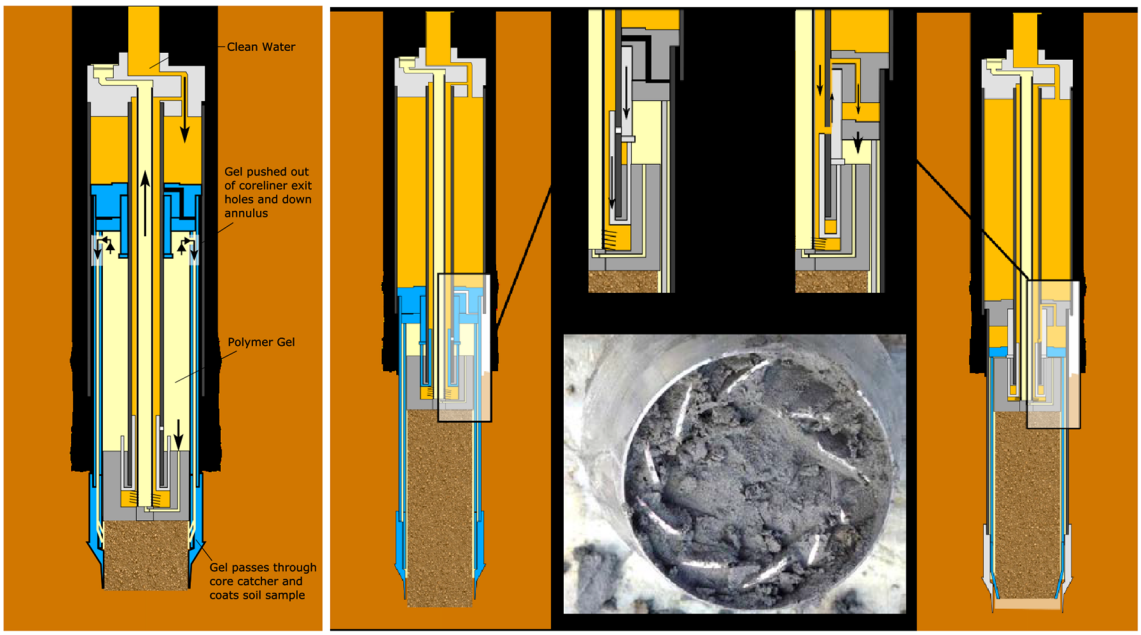

Fig. 13 GP-S during drive phase and core catcher activation (adapted from [66])

the tool is intended to coat the sample. The excess gel must, therefore, be vented from the tool to prevent large pressures being exerted onto the sample. This takes place through the fixed piston allowing the gel to pass through its upper face and enter a small diameter conductor pipe within the fixed piston shaft and exit into the borehole through the top of the tool. Once the tool has advanced 1 m, the base of the traveling piston assembly comes into contact with the spring-loaded pins on the fixed piston. When these pins are depressed, the fixed piston sleeve is moved downwards, opening an exit port on the fixed piston shaft which allows fluid to reach the area between the

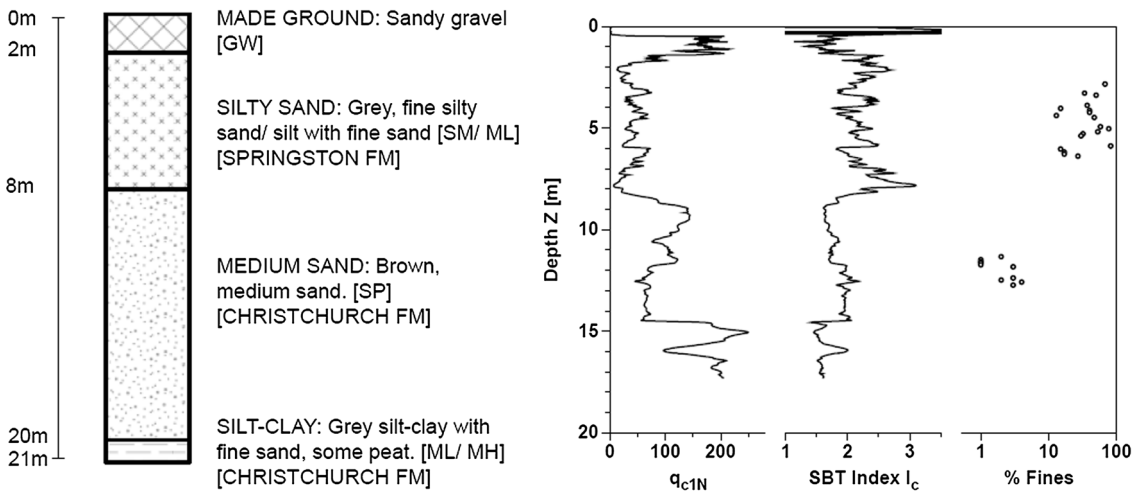

Fig. 14 Summary of borehole K1 and adjacent CPT profile (q_{c1N}, soil behavior type Index I_c and measured *FC* of GP samples) (after [72])

upper and lower traveling pistons. Fluid pressure now acts at the interface between the two traveling pistons and causes the lower traveling piston to apply a downward-acting load on the core-liner barrel, which is transferred to the core catcher. This load causes the core catcher to move downwards, while chamfered the inner surface of the cutting shoe, forcing the core catcher blades inwards, securing the sample within the barrel (Fig. 13). Finally, as described by the authors, at the end of sampling, the fixed piston remains entirely within the core-liner barrel, and in the case of 100% recovery, a 92-cm-long sample will be obtained. In this reported work, a complete similar description of the operation of GP-Tr sampler can be read.

The sample quality of the samples obtained with these Gel-Push systems may be examined visually as these samples reveal a remarkable surface appearance, but for more qualitative evaluation, shear wave velocities or shear modulus are better indicators, as demonstrated above in residual soils. In Christchurch, following the intense work developed after the 22 February 2011, and 13 June 2011 earthquakes, novel Gel-Push sampling was employed to obtain high-quality samples sands from the Central Business District, at sites where liquefaction was observed [72]. GP-D was adopted to obtain high-quality undisturbed samples. Since the combination of shearing and loss of confining stress during sampling may cause irreversible changes to the fabric of the sample (destructuring) and result in a loss of aging effects, a reduction in shear wave velocity measured, Vs (lab vs. field measurements), can indicate the quality of the samples. Based on such assessments, high-quality samples of silty sands were obtained from one of the two examined sites, but the other site had much poorer quality samples recovered. Taylor et al. [72] focusses on the testing of the samples assessed to be of high quality, where little or no loss of aging effects (and subsequently no gross deformation and change in void ratio) is thought to have taken place due to sampling. From observations at the ground surface, the extensive sand boils at the site comprised gray silty sands, typical of the soils encountered between 2 and 8 m depth (Fig. 14) of the Springston Formation. These materials are considered to be typical of flood overbank deposits in the CBD that were deposited during episodes of flooding through Christchurch via gravel channels.

GP samples were obtained from this unit between 3 and 7 m depth, and also in clean medium sands between 10 and 13 m depth. The clean sands are considered to be typical of marine sands associated with shoreline migration following the last glaciation (deposited <7000 years ago), attributed to the Christchurch Formation. Photos of typical samples obtained are presented in Fig. 15 [72].

Sample preparation

According to the description of [72], prior to testing, samples were extruded from the PVC sample tube liners (71 mm internal dia.) and cut to length (~120 mm) before trimming as a 100 × 50 mm cylinder (height × dia.) using a sharp straight edge blade. As the samples were cut progressively as they were extruded, some samples exhibited transitions between more and less silty and sand-dominated layers, featuring fine laminations or indeed lenses of silt at ends or middle of otherwise fine sand-dominated samples. Following the authors' description, these variations are to be expected as part of the natural variability of the deposit, which occurs when the grains fall out of suspension under declining hydraulic gradient, and may represent different flood events. Figure 16 shows the harvesting and trimming operation, with excellent preservation of the natural soil structure (i.e., Fig. 16c). The trimmed samples were

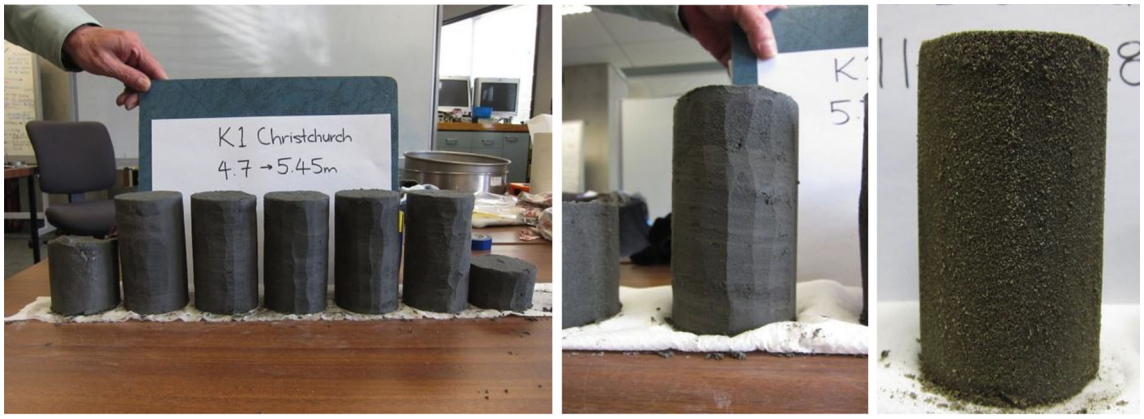

Fig. 15 **a** Typical Gel-Push samples of Springston formation silty sands recovered from one sample tube in borehole K1, **b** close-up of a silty sand sample, **c** typical GP sample of Christchurch Formation marine beach/dune sands (after [72])

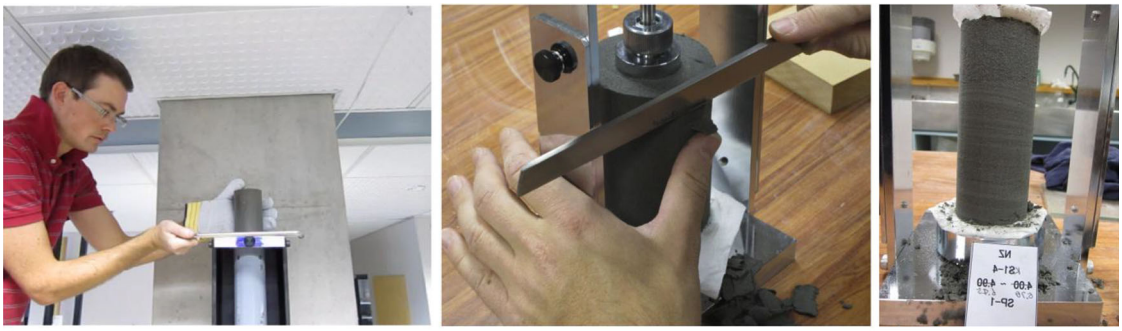

Fig. 16 Preparation of the specimens as illustrated in [72], **a** cutting samples to size with wire saw, **b** trimming, **c** specimen showing natural soil structure

weighed and measured with a vernier, and a sample membrane applied over the sample, before placement in the triaxial apparatus. Samples were saturated, first with CO_2, followed by de-aired water, with Skempton B values in excess of 0.97 typical. A back-pressure of 200 kPa was adopted to facilitate good saturation of the samples.

As described by Taylor et al. [72], the liquefaction triggering strength was based on penetration resistance and the resistance measured using GP sample data. Figure 17a presents the [28] liquefaction strength curves and CRR15 (field) data points corresponding to the cyclic strength curves. The width of the error bars indicates the variation in q_{c1N} over the sampling depth. Figure 17b presents the same plot but with GP sample points derived from alternative cyclic strength curves. The errors in q_{c1N} are much reduced as the CRR15 at a single corresponding depth point of the individual samples that comprise the curves are used here to convey variance, rather than a depth range as before. However, to some extent the reduced variability is on account of the sorting process (e.g., high fines contents typically have lower q_{c1N}). Some points when sorted for soil type generally match the expected position on the Idriss and Boulanger empirical curve, e.g., points 2 and 3 are somewhat parallel to the 15% FC curve, and point 1 is further to the right as it is of both lower FC and higher density, whilst point 4 situated to the left of the plot represents higher FC and lower density. Points 5, 6, and 7 again appear as outliers within this plot, consistent with earlier noted concerns about these test results. In general, the silty sand material consistently plots below the cyclic strength predicted by the semi-empirical method, which may be on account of the uncertainty inherent in the development of the curves, particularly for sands with fines.

Case of sampling at Zelazny Most, Poland, copper tailings disposal depository

Jamiolkowski [31] report on comprehensive geotechnical site investigations, carried out over a period of two decades, at one of the world's largest copper tailings disposal reservoirs, located in Zelazny Most, Poland. In view of the

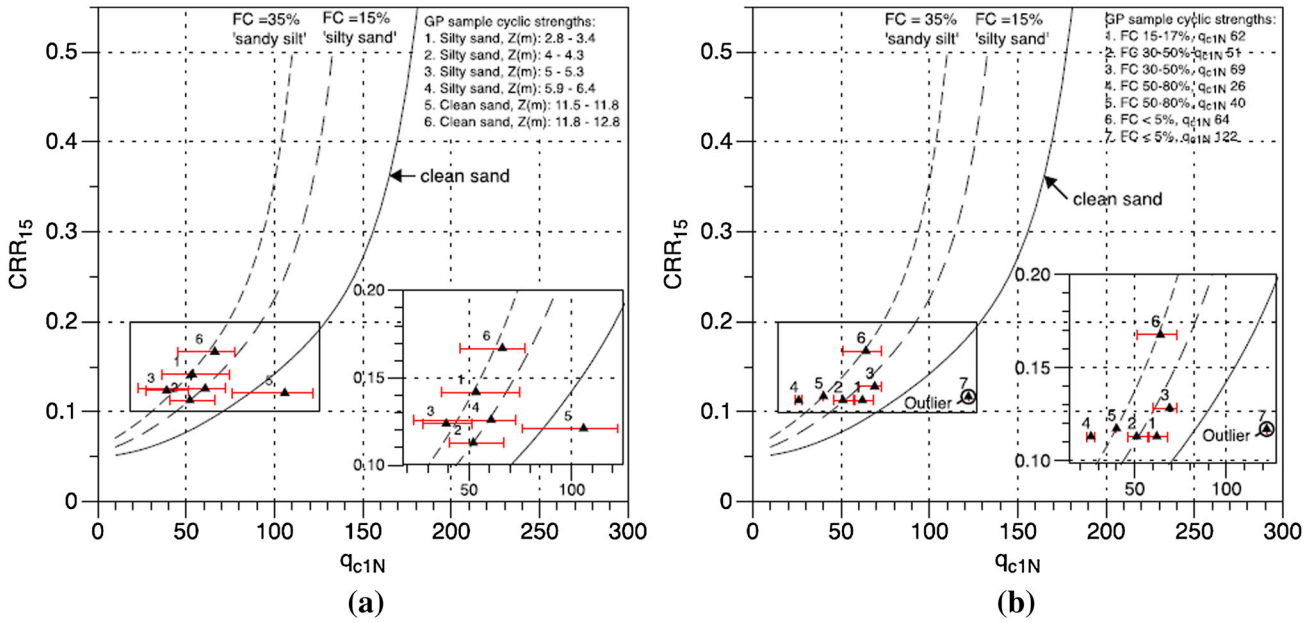

Fig. 17 **a** Comparison empirical liquefaction triggering curves of Idriss and Boulanger (after [28]) and GP sample *CRR15* by depth and, **b** by soil type hierarchy. Corresponding q_{c1N} values from adjacent CPT

difficulties associated with obtaining undisturbed samples of silt and silty sand at the tailings depository, the investigation relied primarily on in situ tests including S-CPTU; S-DMT; cross-hole tests, and block sampling. In 2013, a GP-Tr sampler was brought in and succeeded in obtaining quality samples. Figure 18 shows the zone of gradation curves of the tailings disposal at location 7E−8E, close to where the GP-Tr samples were obtained. One of the gradation curves of the GP-Tr samples, taken at the site, is also shown. The specific GP-Tr sample used appears to be sandier than the surrounding area.

Figure 19a shows the shear wave velocities determined by cross-hole tests at location 7E−8E, and the shear wave velocities measured in the laboratory using GP-Tr samples. The figure also shows the measurements normalized at 98 kN/m^2 to remove the effect of overburden pressures on the shear wave velocities. A good overall agreement seems to exist between the in situ and laboratory measurements. The normalized shear wave velocities were replotted by Mori and Sakai [48] to show the ratio of the velocities in the laboratory to in situ against the normalized in situ velocities, see Fig. 19b. This figure clearly demonstrates the relative difference between the two normalized velocities. All the data lie between normalized in situ velocities of 200 and 300 m/s. However, the ratios of normalized shear velocities show a wide scatter, falling between 0.5 and 1.3, and indicating a possible divergence in the sample quality. In general, samples having shear wave velocity ratios close to unity are considered to be of high quality. It is, however, noticeable that many of the

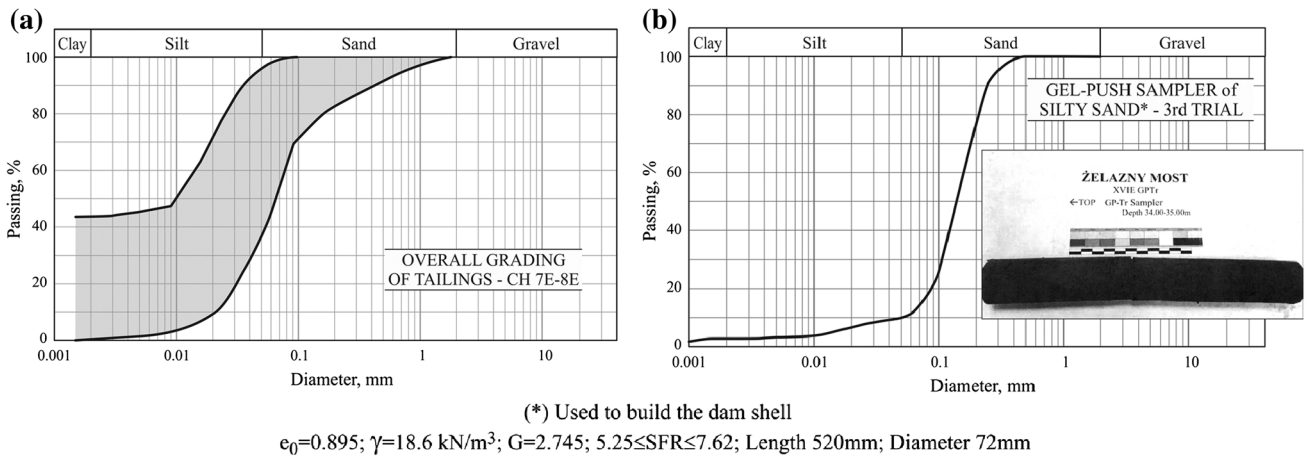

Fig. 18 Gradation curves of tailings at 7E−8E and GP-Tr sample (after [31])

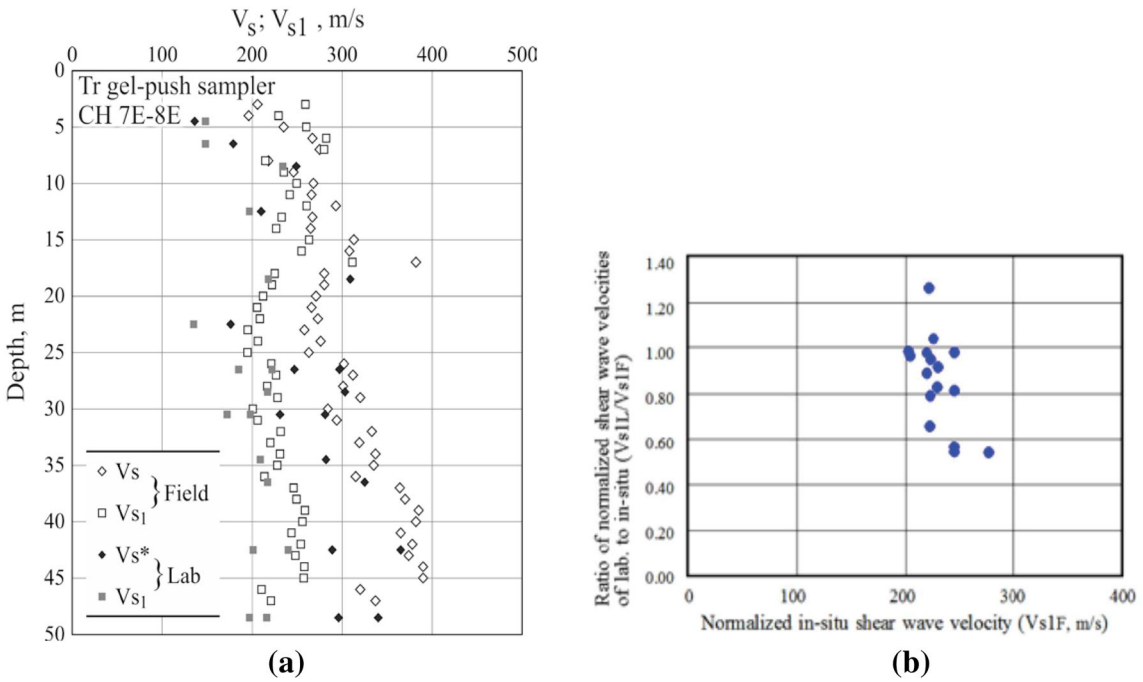

Fig. 19 **a** East dam. Comparison of V_{s1}(F) vs. V_{s1}(L). (*Asterisk*) Bender element test (after Jamiolkowski [31]); **b** ratio of normalized shear wave velocities of laboratory to in situ vs. normalized in situ shear wave velocity (as reanalyzed by Mori and Sakai [48])

data points lie between 0.8 and 1.0, indicating these samples retained high quality.

The comparison between the stress paths of static and cyclic loading tests using those samples has shown ratios close to unity, with those having very large or small values to examine the possibility of sample disturbance. Since block sampling has been conducted on the site, it may also be of interest to compare the strength and stress paths of the GP-Tr and block samples, as block sampling can preserve soil characteristics in situ (Mori et al. 1979). As emphasized by Mori and Sakai [48] the sample quality of the GP-R and GP-D samples may be examined visually as these samples reveal a remarkable surface appearance, but for more qualitative evaluation, shear wave velocities or shear modulus proved more clearly, since they prove to be better indicators, that the GP-Tr and GP-S samplers are the latest additions to the GP family and have shown remarkable capability in sampling hard to obtain silt, silty sand, and sand. The polymer coating mechanism is an innovative key factor and an excellent solution to the inabilities of previous samplers.

A compromise for sands with fines

In another work from the same group in the University of Canterbury, Markham et al. [46] have shown that it was possible to obtain high-quality samples sands from the Central Business District using the Osterberg-type hydraulic fixed piston thin-walled sampler (the Dames and Moore, DM, sampler) for most of the predominantly silty and silty sand soils. Figure 20 shows the general setup and operation of an Osterberg-type hydraulic piston sampler, as included in ASTM D6519-08 [4].

This sampler uses a constant inner diameter smooth brass tube with a relatively low area ratio of 7.6%. These features of the sampling tube coupled with the relatively short advancement length (45 cm) provided a means for retrieving high-quality samples of silty soils and medium dense sands.

Markham et al. [46] have shown that shear wave velocity (V_s) determined on select number of specimens allowed to compare V_s-Lab and V_s-Field, being the results from these comparisons yielded reasonable trends with regard to V_s-Lab/V_s-Field ratios, as for the densities (void-ratios) determined in the lab specimens and in derived from correlations with in situ tests results. The results in very loose and loose, relatively clean sands (SP and SP-SM) were the exception. In this case, the test results indicated that the sampling and testing procedures densified these soils.

Sampling and sample quality assessment in soft soils

Soft soil deposits

Three natural soil deposits are used in this paper to describe main aspects of the sampling process as well as the

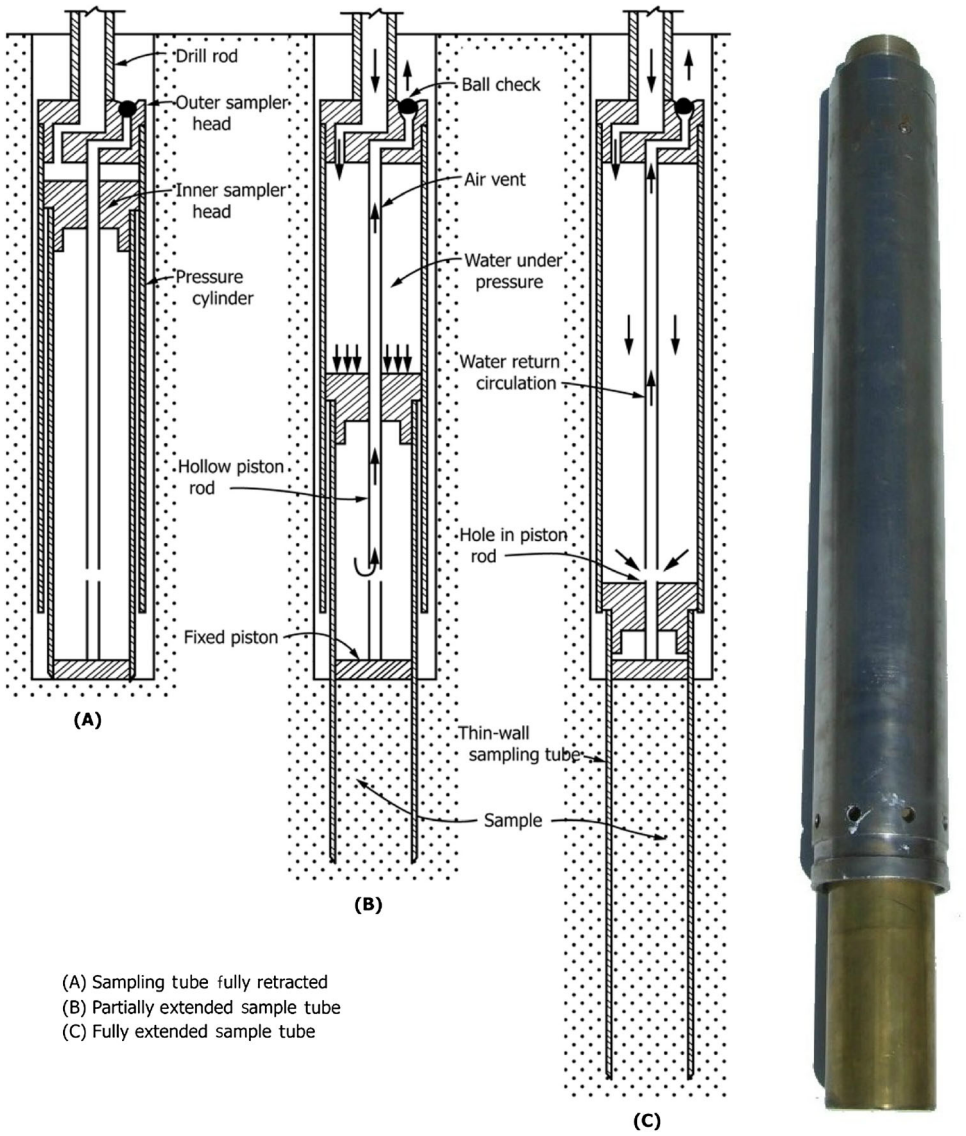

Fig. 20 Schematic of hydraulic piston sampler operation using a thin-walled sampling tube (from ASTM D6519-08 [4])

assessment of sample quality in soft soils. The soils described below correspond to the low-plasticity silty deposits from Llobregat River in Barcelona (Spain), the low-plasticity silty clays and clayey silts from Castelló d'Empuries (Spain) as well as the high-plasticity estuarine soft clay deposits from Ballina, New South Wales (Australia). A brief description of each soil profile is given below.

Silty deposits from Llobregat River (Barcelona, Spain)

The deltaic deposits of the Llobregat River in Barcelona (Spain) are composed by medium to soft soils of Holocene age that, at large scale, constitute a rather homogeneous geological formation. Figure 21 shows the soil profile at the Virgen de Monserrat Station of the new Metro Line (L9) where this formation appears. The soil profile at the site comprises a top layer of made ground about 1.5 m thick, overlying 4 m of brown fine sandy silts. Around 10 m of slightly gravelly gray fine sands appear below. These, in turn, are underlain by a gray layer of silty clays and clayey silts finely interbedded with sands, sandy silts, and clays (see Fig. 20a). Figure 20b shows a CPTu profile of the site.

The profile reveals that the layer composed by silty clays and clayey silts is typically interbedded with coarse layers whose frequency decreases with depth. Soil characterization carried out by Pineda et al. [55] on a block specimen of silty clay retrieved from −13.5 m.a.s.l. shows a fine fraction higher than 99% (% <2 μm ranging between 21 and 34%). Correspondingly, the silt fraction varies between 66 and 79%. The liquid limit and plasticity index are equal to 34% and 14%, respectively. Thus, the fine fraction is classified (USCS) as a low-plasticity clay (CL).

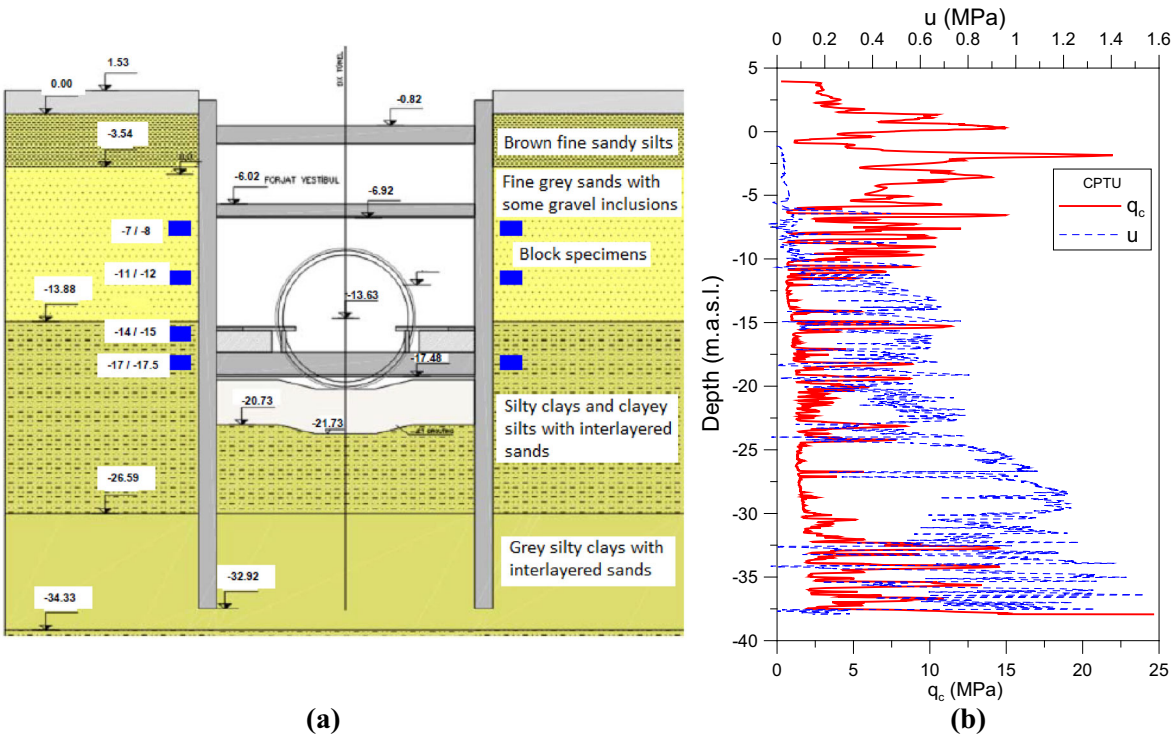

Fig. 21 Soil profile and CPTu profile at Virgen de Montserrat Station (Barcelona) [55]

The density of solids, ρ_s, ranges between 2.71 and 2.73 Mg/m^3.

Deltaic deposits from Castelló d'Empuries (Costa Brava, Spain)

Castelló d'Empúries lies in the flat central section of the Costa Brava (Spain) located between the Paleozoic Pyrineic relief and the Mesozoic Montgrí massif. This is an alluvial plain mostly formed by deposits of the rivers Fluvià and Muga which originate a typical Mediterranean deltaic ambient (see Fig. 22a) [14]. Holocene deposits reach here a thickness of about 20–30 m in the area, alternating between sand-dominated deposits (e.g., dunes) and silt–clay deposits (coastal marsh). The testing site is flat and lies at about 10 m above the local datum, having a roughly rectangular shape of 30 by 50 m. The water table oscillates regularly between 1.5 and 3.6 m depth. Grain size distribution analysis from samples recovered in a continuous borehole allows identifying a sequence of fine and granular soils that is characteristic of these deposits.

Figure 22b shows the tip cone resistance curves. The profile reveals two soft levels with $q_c \leq 2.5$ MPa (from 2 to 6 m depth and from 12.5 to 15 m depth) separated by a stronger granular level. As indicated in this figure, sampling took place in the two soft levels. Soil characterization carried out using Sherbrooke specimens [63] showed that these silty deposits present a fine fraction ranging from 60 to 97%. These materials classify as low-plasticity clays (CL) with clayey fractions ranging between 14 and 29%. The density of solids, ρs, ranges between 2.63 and 2.68 Mg/m^3.

Estuarine soft clays deposits from Ballina site (New South Wales, Australia)

Natural estuarine soft clays are commonly found along the eastern and southern Australian coastlines. The establishment by the ARC Centre of Excellence for Geotechnical Science and Engineering (CGSE) of a National Soft Soil Testing Facility (NFTF) at Ballina, New South Wales, [34] has allowed high-quality in situ testing and monitoring, combined with advanced laboratory testing, to characterize a typical Australian estuarine soft clay with the goal of improving engineering design methods. The stratigraphy at Ballina site comprises the alluvial crust ($z < 1.5$ m) which is underlain by the Ballina clay ($1.5 < z < 11$ m), a transition zone with increasing sand content, sand ($11 < z < 14$ m), and stiff clay ($z > 15$ m). Ballina clay represents the estuarine soft clays (Holocene age) of high to extremely high plasticity commonly found along the east Australian coastline. The natural clay is structured and lightly over-consolidated (YSR <2). It has an organic content of around 3% and soil activity equal to 1. The main mineral components are kaolinite, illite, quartz, illite/smectite, and amorphous minerals. Detailed

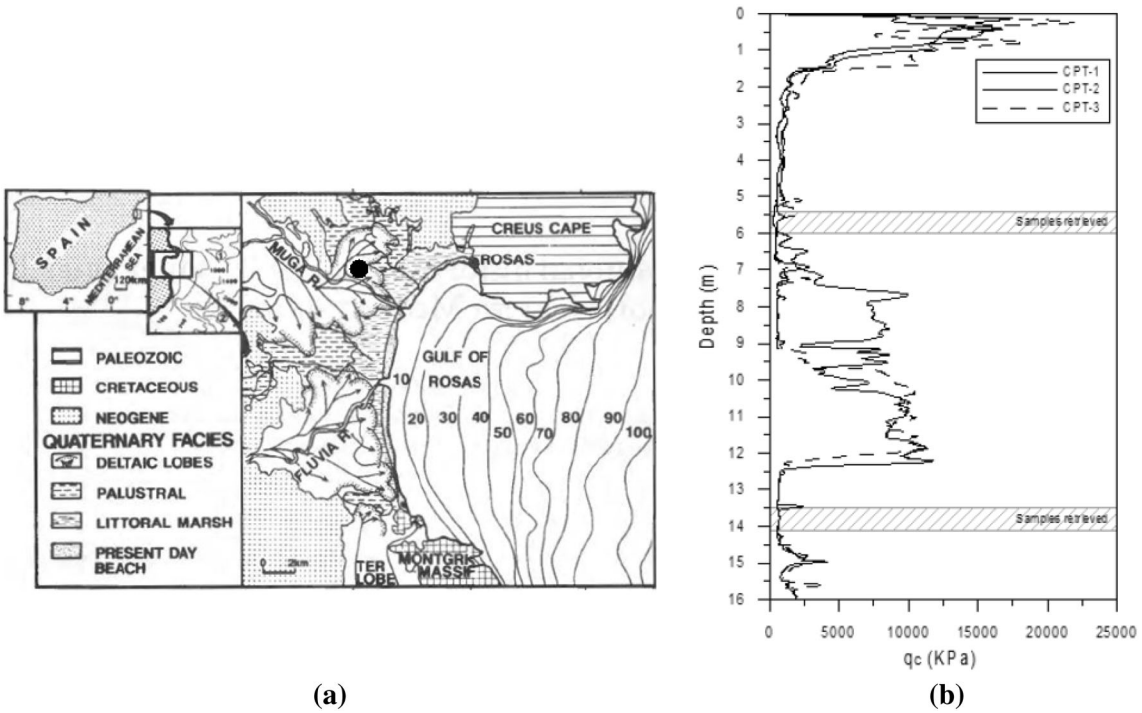

Fig. 22 **a** Location of the test site at Castelló d'Empuries (from Díaz and Ercilla [14]). **b** CPTu profile at the test site [63]

characterization of the natural Ballina clay is given by Pineda et al. [58]. Figure 23a shows the profiles of natural water content, Atterberg limits, particle size distributions, and electrical conductivity estimated for specimens obtained from boreholes Inclo 2 and Mex 9, 50 m away from each other. The natural water content increases with depth from 20% up to 120%. Differences between the liquid limit and natural water content are less than 10–15%. The plastic limit ranges between 20 and 53%, whereas the liquid limit varies from 55% to 135%. The particle size distributions show differences between the boreholes at shallow depths ($z < 2$ m), mainly in terms of the sand content. The clay content is predominant below 2 m, with maximum values of up to 82% while the sand content lies around 1%. The presence of salts in the pore fluid is one of the fingerprints of marine clays, which also play a key role on their mechanical response. Bulk (fluid + solids) and the pore fluid salinity measurements were carried out on Ballina clay. A similar trend is observed between EC_{bulk} and EC_{fluid} with depth. The bulk measurements vary with depth from 4 to 15 mS/cm. The values of EC_{fluid} are larger than EC_{bulk}, and vary from 7 mS/cm up to 36 mS/cm (the average below 5 m). Figure 23b, c shows q_c and u profiles, respectively, obtained from CPTu testing at four locations in Ballina site. The good agreement between these profiles confirms the homogeneity of the soft clay layer ($0.15 < q_c < 0.45$ MPa) which is located between 1.5 and 11 m depth.

Sampling techniques

Block sampling

Two main sampling techniques are commonly used in practice: block and tube sampling. The first method provides (a priori) soil specimens of the highest quality due to the less mechanical deformation involved in the cutting/carving process. However, this procedure is usually limited to shallow depths (trial pits, shafts, and shallow excavations) where the water level is kept below the sampling depth and the stability of the ground may be ensured without requiring expensive temporal stability measures. Hand-carving blocks are good option in soft cohesive soils. Although textbooks suggest carving rectangular block samples, cylindrical specimens are more convenient as this shape provides more stability during the cutting process.

The process followed during a block sampling in the deltaic deposits of Llobregat River described in "Natural soils with highly sensitive structural features" is shown in Fig. 24. Working from the excavation bottom, the block sample was hand carved using a sharpened spatula to trim a 1-m-side square plinth into a cylindrical specimen of approximately 360 mm diameter and 300 mm height. The trimming process was slow but easy due to the soft nature of the soil. The cylindrical shape was convenient to avoid sharp edges. The block specimen was covered with several layers

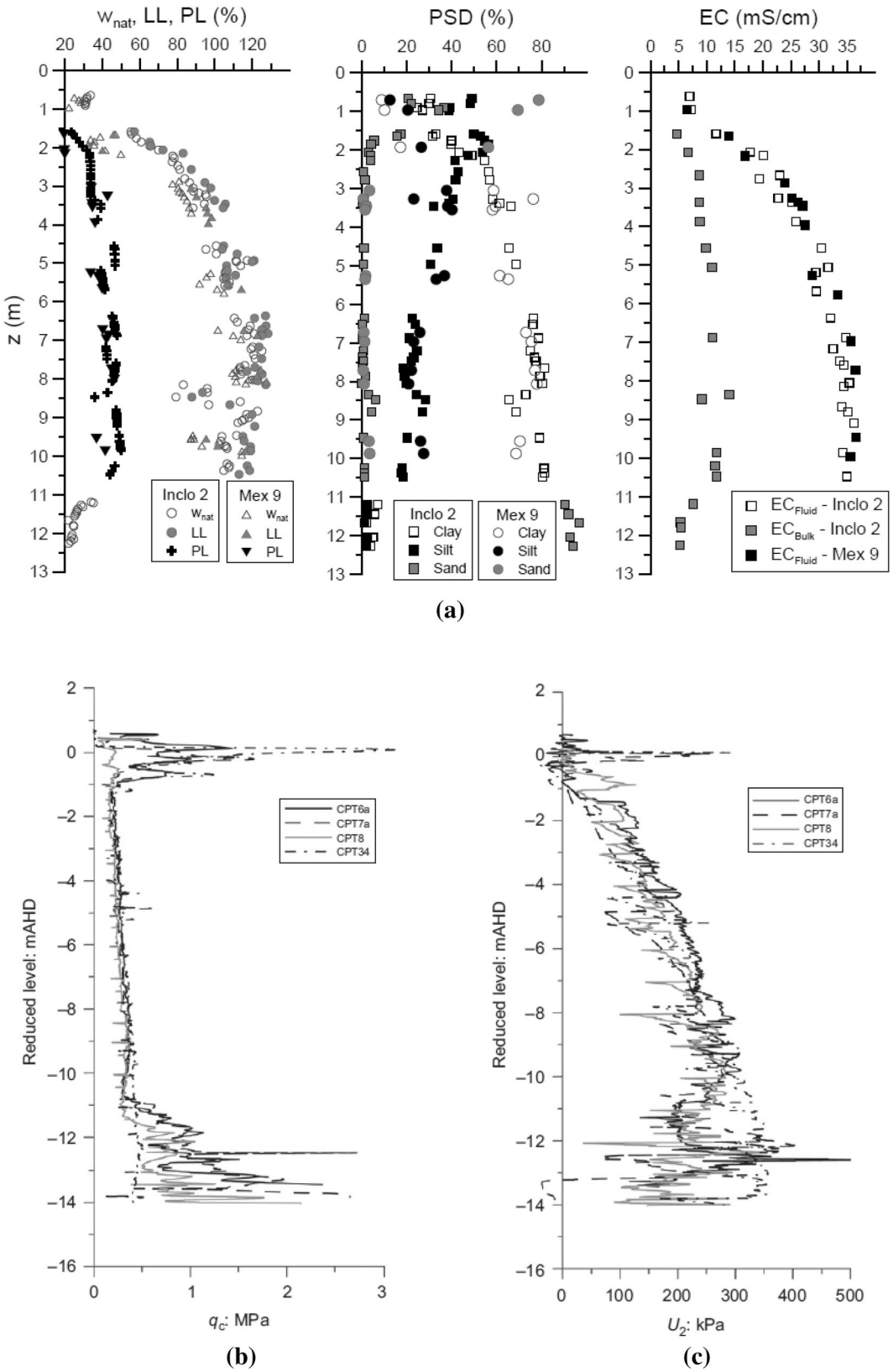

Fig. 23 Geotechnical characterization of Ballina clay. **a** Index properties [58]. **b**, **c** CPTu profiles from the estuarine deposits at Ballina site [34]

of plastic wrap and foil seal to avoid moisture losses. A PVC tube (400 mm in diameter) was used to protect the sample laterally. The inner space between the sealed sample and the tube was filled with paraffin wax ($T \approx 55$ °C) to isolate the block during transportation and storage at the laboratory. For handling purposes, the sample was sandwiched between two PVC plates externally doubled by two 8-mm-thick steel plates. Four-threaded steel bars at the corners were used to press the plates against the tube (Fig. 24). Block specimens were placed on foam and wood plates for transport and storage in the laboratory.

To overcome the issues related to the limited sampling depth of hand-block carving, mechanical methods are required. The Sherbrooke sampler [41] is, to date, the mechanical sampling technique capable to produce specimens of the highest quality in soft soils, including quick clays, sensitive clays, silty clays, silts, and peats (e.g., [25, 43, 44, 59, 63]; among others). This technique requires pre-drilling a 400-mm borehole to around 500 mm above the sampling depth. Although the borehole is commonly filled with water or mud, casing is sometimes required (typically in low-plasticity sandy soils) to avoid instability problems. An auger and flat cutter are used to penetrate the last 500 mm prior to connecting the sampler to the drill rig. The Sherbrooke sampler is a metallic cage made of stainless steel capable of carving 250-mm-diameter specimens using horizontal cutters and a set of three blades located at the bottom of the sampler. Each cutter includes water jets to help to evacuate the remoulded soil (Fig. 25). The sampler rotates at low angular speed (5 r.p.m.) to minimize soil disturbance. After carving a cylindrical specimen of around 350 mm in height, the bottom blades (initially locked in open position) are activated from the ground surface to cut the base of the sample. This set of blades provides support to the block specimen during sampler retrieval.

Figure 26 shows the sampling process using the Sherbrooke sampler in two soft soil deposits: the low-plasticity silty deposits from Castelló d'Empuries as well as the high-plasticity Ballina clay described above. Block specimens are placed on rigid and waterproof platforms. Block sealing combines plastic film and aluminum foil to avoid moisture losses. It also minimizes the effects of thermal gradients caused by waxing. Extra care is needed to handle block specimens. Therefore, extra tools are required for carrying the blocks in situ and in the laboratory. Blocks are placed inside plastic containers, on a layer of wet sand or sawdust, which may be filled up with strips or foam chips to provide lateral confinement during transport and sample storage (see Fig. 26). Under controlled room conditions and ensuring the good performance of the sealing method, block specimens can be stored for several months prior to testing. The phenomenon of moisture redistribution inside the specimens is the factor to evaluate in all cases and particularly when soil specimens are tested after long-term storage.

The main drawback of the Sherbrooke sampler is its operational cost which makes it attractive only in special projects or for research purposes. This sampler has been recently redesigned at NGI (Norway) to make it more competitive against conventional tube sampling techniques. The upgraded device, called the Mini Sherbrooke sampler [18], still provides a truly undisturbed block specimen (160 mm in diameter and 300 mm in height) which is fundamental for high-quality laboratory testing. The new design requires the drilling of a 200-mm borehole which fits properly with standard drilling methods used in geotechnical practice.

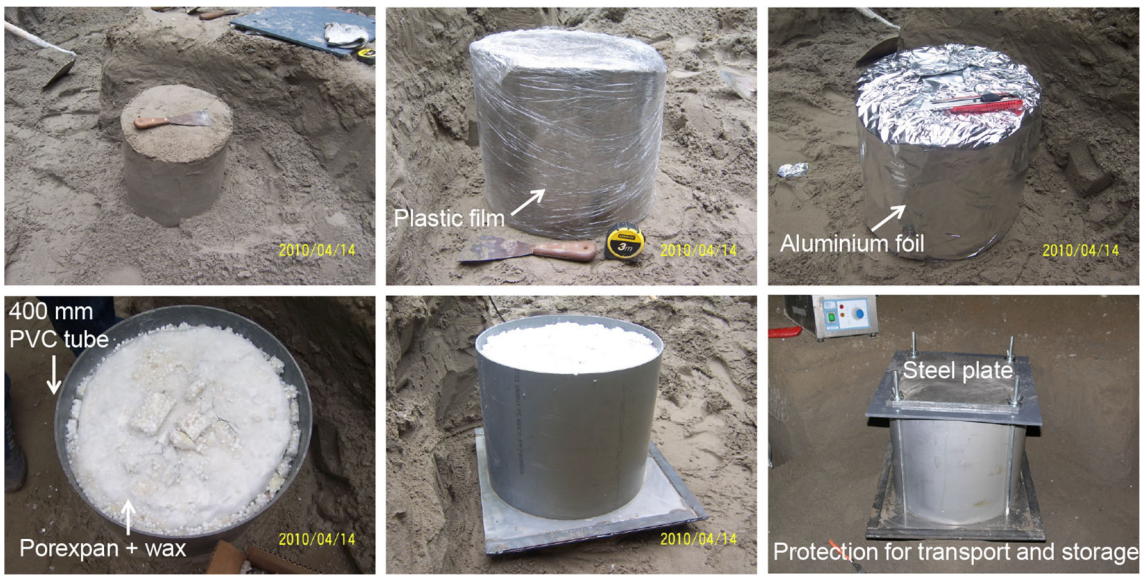

Fig. 24 Block sampling in silty deposits from the Llobregat River, Barcelona (Spain)

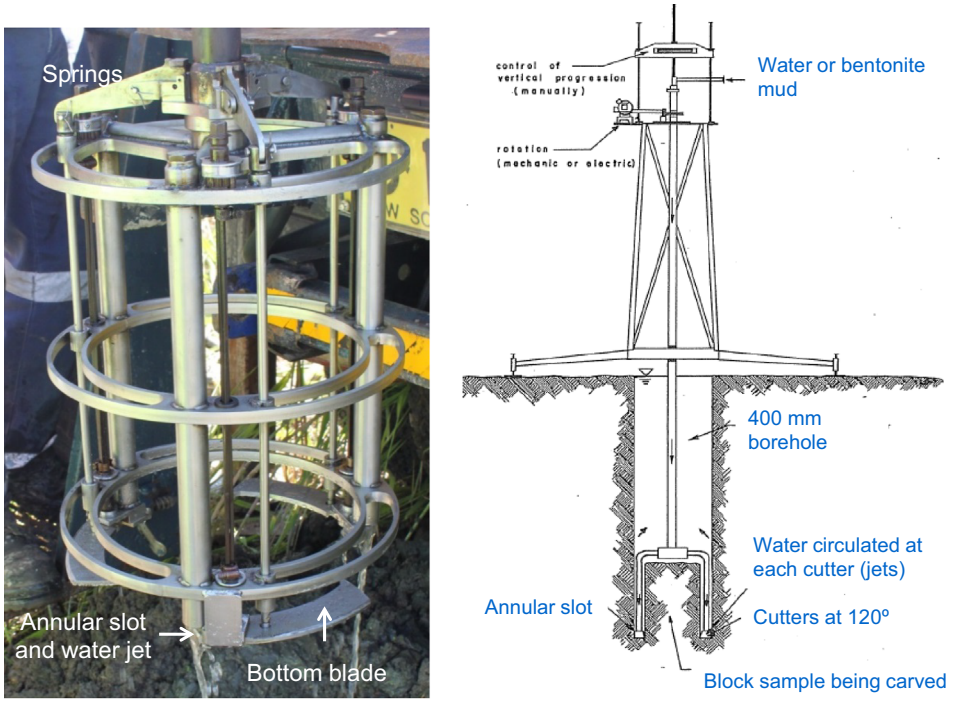

Fig. 25 The Sherbrooke sampler [41]

Fig. 26 Sherbrooke sampling campaigns in silty deposits (Spain) and soft clay (Australia)

Tube sampling

A wide variety of tube samplers is available for sampling soft soils. These are pushed (drive) into the ground from the bottom of a borehole. Drive samplers can be divided into three main categories (e.g., [9]): (i) open samplers, (ii) piston samplers, and (iii) sliding liners samplers. Figure 27 shows the main features of open samplers and fixed piston samplers which are described below.

The open sampler, particularly Shelby tube, still remains as the most common sampling method in soft soils due to their simple operational principle (Fig. 27). However, specimens retrieved using Shelby tubes are largely affected by mechanical deformation mainly at the upper part of the

sampler as a consequence of the entrance of disturbed soils from the bottom of the borehole. Another issue is the difficulty of the check valve to maintain the vacuum during sampler retrieval which affects the total recovery. Baligh et al. [6] studied the undrained penetration of a rigid open sampler (S sampler) in saturated clay using the strain path method [5]. Neglecting the differences in the geometry of the cutting edge between the S sampler and open (Shelby) tubes, it was shown that (see Fig. 28a) (i) large shear strains (and strain non-uniformity) take place in the outer zone of the tube, mainly at the soil–tube interface, and (ii) the vertical strain component is dominant at locations closer to the centreline. Three deformation stages were identified for soil located at the centreline of the sampler: (a) compression, ahead of the sampler, (b) extension, near to the cutting edge, and (c) compression, inside the sampler. Clayton et al. [8] complemented the work done by Baligh and co-workers by considering more realistic geometries for the cutting edge of the sampler. The results were analyzed in terms of the geometric descriptors introduced by Hvorslev [27] to quantify the effects of tube sampling caused by different tools. They showed that the area ratio (AR = area of the annulus of the tube sampler divided by the area of the tube specimen), as well as the angle of the cutting edge (α), dominates the compression component ahead of the sampler (see Fig. 28b, c). The axial compression increases with the increasing of AR and α. On the other hand, the inside clearance ratio (ICR), which refers to the enhancement of the internal tube diameter behind the cutting edge, has a strong influence on the extension component inside the sampler. In summary, two main deformation mechanisms take place during tube sampling in soils. Large shear strains develop far from the centreline at locations closer to sampler wall, whereas vertical compression is the dominant mechanism near the centreline.

The appearance of the hydraulic fixed piston sampler [54] catalyzed the development of several devices of its kind worldwide during subsequent decades. Although its working principle of the hydraulic fixed piston sampler is a bit more complicated than the Shelby sampler, it is still simple enough to be adapted to conventional practice without major modifications (Fig. 27). The main differences between these two samplers are: (i) the presence of an internal fixed piston to prevent the entrance of disturbed soil during lowering to the sampling depth, (ii) the presence of an internal thin-walled tube sampler that is pushed into the ground using a floating piston via hydraulic pressure. After full penetration, the hydraulic fluid flows up (through the hollow piston rod) and down (through the cutting toe) to ensure the same static pressure inside the sampler and at the bottom base. It helps to minimize suction at the bottom of the sampler during withdrawal (Fig. 27). The NGI 54-mm sampler [1] and the JPN 75-mm sampler (e.g., [71]) are examples of fixed piston type samplers that have been incorporated into the current practice in Norway and Japan, respectively, due to their lower soil disturbance compared with Shelby tubes and free-piston samplers.

An innovative piston-pneumatic-injection sampler (IGS sampler) specifically designed to maximize sample retention and reduce sample disturbance in soft soils is described by Pineda et al. [57]. The stainless steel sampling tube has an

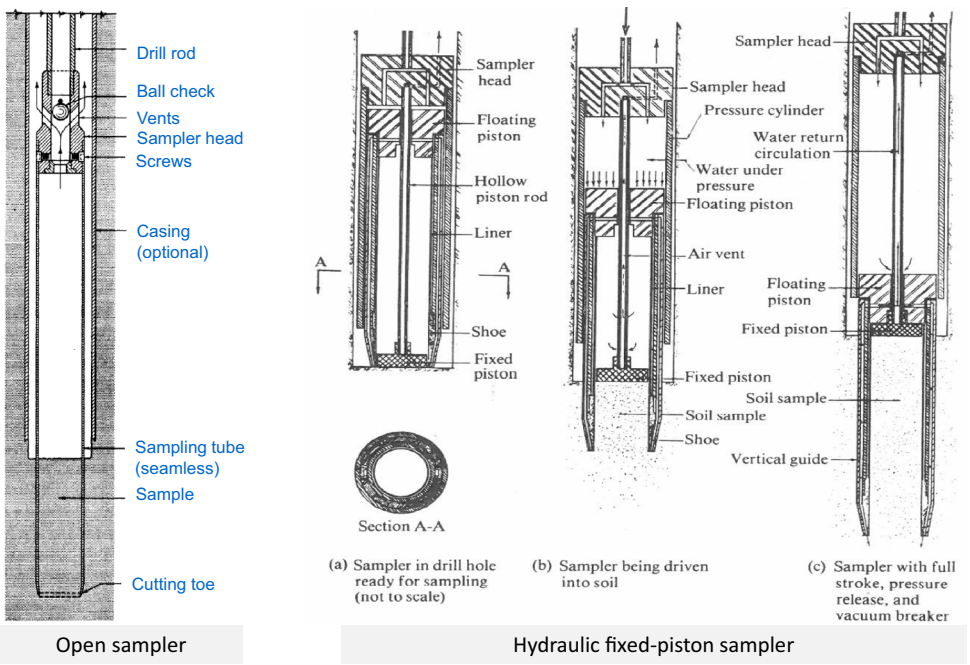

Fig. 27 Shelby tubes and hydraulic fixed piston sampler (from Clayton et al [9])

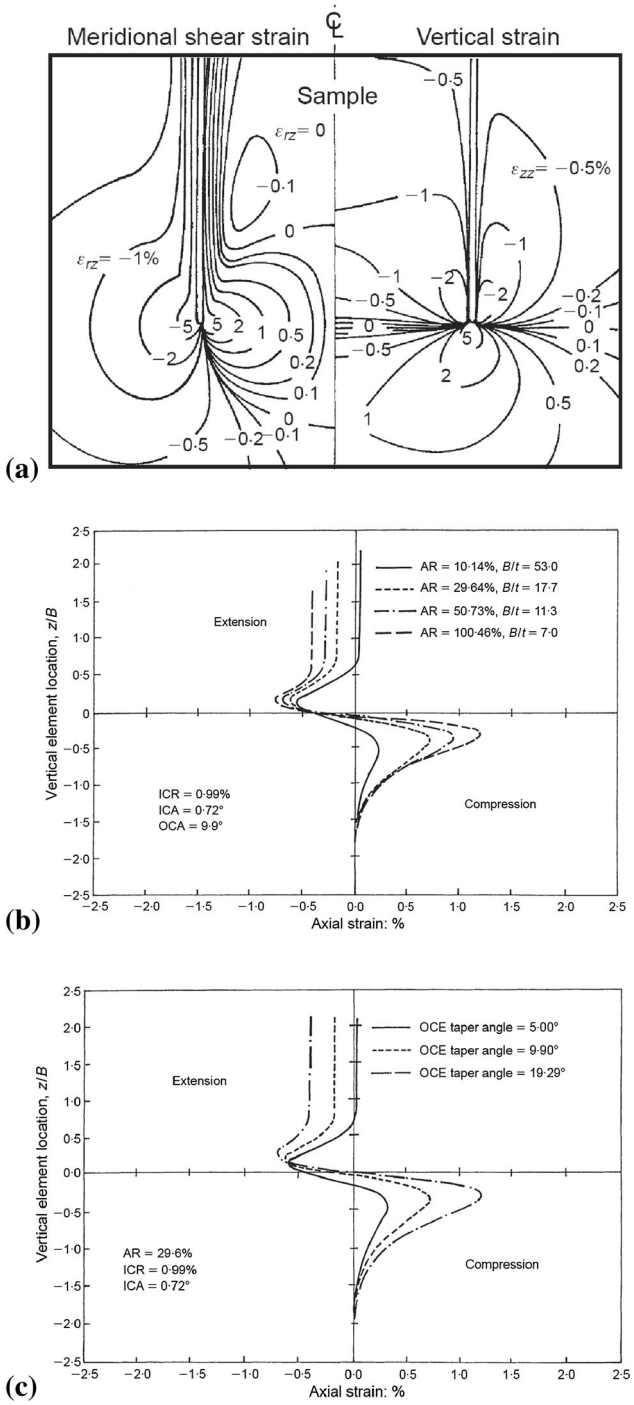

Fig. 28 Deformations during undrained tube sampling in saturated clay. **a** Shear and vertical strains (from Baligh et al. [6]). **b** Influence of AR on centreline vertical strains. **c** Influence of ICR on centreline vertical strains (from Clayton et al. [8]

outer diameter of 63 mm, length of 880 mm, a wall thickness of 1.6 mm, and a 5 degree cutting edge. The area ratio is 11%. The operation principle is schematically shown in Fig. 29. The tube is closed using a conical fixed piston inside the tube during advancement into the soil to the top level of the sampling depth. Advancement to sampling depth is made by direct pushing using a CPT rig in a similar fashion to pushing a CPT. The piston is then held stationary as the tube is advanced 880 mm into the soil to capture the sample. The sampling tube is advanced over the stationary fixed piston using a specially designed cylinder behind the tube, actuated by water pressure of approximately 100 Bar. The sample in the tube is released from the soil mass below by "cutting" it free with a very brief injection (a "shot") of high-pressure nitrogen at the sample tube cutting face, before it is extracted. Two stainless steel tubes (6 mm in diameter) externally welded to the sampling tube are used to apply the nitrogen directly below the cutting face. As the sample tube is extracted, low pressure air or water is injected into the void below the sampler to eliminate suction while pulling out. The objectives of this procedure are to reduce tension in the sample and to avoid sample loss due to suction. The tube is then unscrewed and pulled off the piston. The IGS sampler has demonstrated very good performance in estuarine soft clays from NSW (Australia), producing specimens of high quality for laboratory testing [57]. Emerging tube sampling techniques are nowadays getting attention from practitioners due to the well-recognized issues of standard methods for obtaining undisturbed

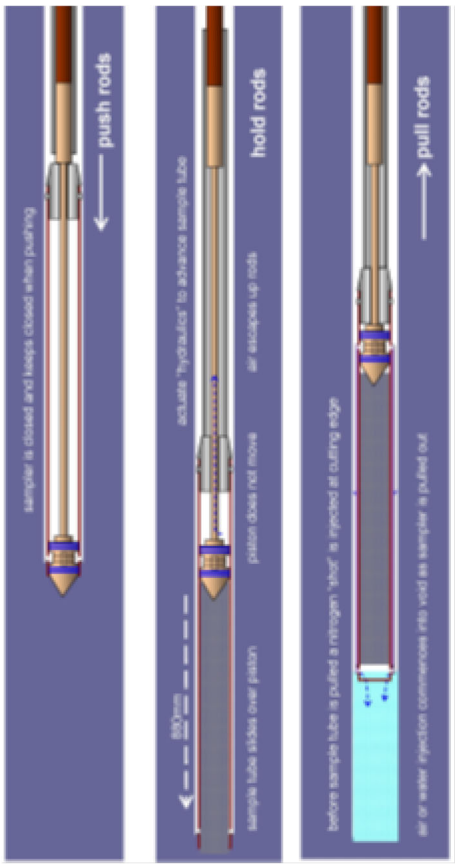

Fig. 29 The IGS sampler [56]

specimens in silty deposits as well as granular soils (clean sands). It is extremely difficult to obtain high-quality specimens in soils with high liquefaction potential like clean sands and some silty soils. The Gel-Push sampler, which keeps the same operational principle as the hydraulic fixed piston sampler (as described above), assumes that the main source of disturbance is due to sidewall friction as the soil enters the tube sampler.

A set of recommendations to properly select tube samplers and minimize mechanical disturbance was given by Ladd and DeGroot [37] (see Table 2). They suggested the use of sampler tubes with ratio B/t (B outer diameter and t thickness of the tube wall) higher than 40, area ratio lower than 10%, no inside clearance ratio, and angle of the cutting shoe lower than 10 degrees. Moreover, they recommended avoiding top and bottom ends in tube specimens ($\approx 1.5\ B$ each) for mechanical testing due to the large degree of soil disturbance. Soil from top and bottom ends should be used for characterization purposes only.

Sealing, transport, and storage of soil specimens

Little attention is commonly given in practice to aspects such as sealing methods, transport, and sample storage despite their potential to affect measured soil properties in a major way. Although other sealing methods have been proposed, waxing remains as the most common procedure used in practice due to its simplicity and low cost. However, thermal gradients generated by waxing when sealing tubes and block specimens may lead to important soil disturbance. This gradient dissipates with time as it hardens, but generates excess pore water pressure under undrained conditions as the pore water is not allowed to drain out. This may cause significant moisture redistribution within the clay, which is not easy to predict in advance. Unfortunately, the recommended temperature for pouring the wax (sometimes not even included in local standards) is not always controlled in situ so that soil specimens are frequently exposed to temperatures much larger than the melting point of the wax, reaching values up to 80 °C. Moreover, biological processes (e.g., methane release) and chemical reactions may also be triggered by thermal fluctuations, but are rarely evaluated in practice. Figure 30 shows the approach followed at the University of Newcastle (UoN) to seal tube specimens of Ballina clay (Sect. "Natural sands and non-plastic silty sands: focus on cyclic instability—earthquake engineering"). After sampler retrieval, tube ends are properly sealed with several layers of plastic film underlying a 10-mm-thick polystyrene (porexpan) plate covered externally with wax (10–15 mm thickness) (Fig. 30a). The porexpan plate is intended to isolate the clay from the thermal gradient caused by wax. Silicone grease is applied at the interfaces between the tube sampler and the porexpan plate for improving sealing. Tube ends are finally covered with plastic lids prior to packing for transport. Specimens are then placed, vertically aligned, in sealed plastic containers on a thick layer of wet sand, which helps to maintain a high relative humidity environment (RH $\approx$99%) and minimize moisture losses. Tubes are packed using scraps of polystyrene (porexpan) to induce lateral confinement and absorb vibrations caused during transport (Fig. 30b). Plastic containers are stored in an industrial fridge under constant temperature conditions ($T = 16$ °C). A fridge is preferred in this case to reduce the likelihood for water condensation to occur which could be absorbed by the clay in the long-term starting undesirable microbiological processes.

Assessment of sample quality

One of the challenges in the study of the mechanical behavior of natural soft soils lies in the selection of 'representative' soil specimens for laboratory testing. Sample disturbance as well as the natural soil variability along the tube, may affect the results of laboratory tests and lead to important discrepancies between in situ and laboratory data. Several methods have been proposed to assess sample quality in soft soils. It includes non-destructive techniques as well as conventional laboratory (element) tests. The most common approaches are based on:

- Volumetric strain and void ratio changes after recompression to in situ effective stress.
- Image analysis (X-ray and CT scans).
- Suction measurements.
- Shear wave velocity measurements.
- Microstructural analysis.

A brief description of each approach is given below.

Volumetric strain and void ratio after recompression to in situ vertical effective stress

Different criteria have been proposed over the last decades to evaluate the sample disturbance of soft soils. The proposals by Andersen and Kolstad [1] (see also [73]) and

Table 2 Recommended criteria for the selection of tube samplers [37]

B/t	Area ratio, AR (%)	Inside clearance ratio, ICR (%)	Angle of the cutting shoe, α (°)
>40	<10	0	<10

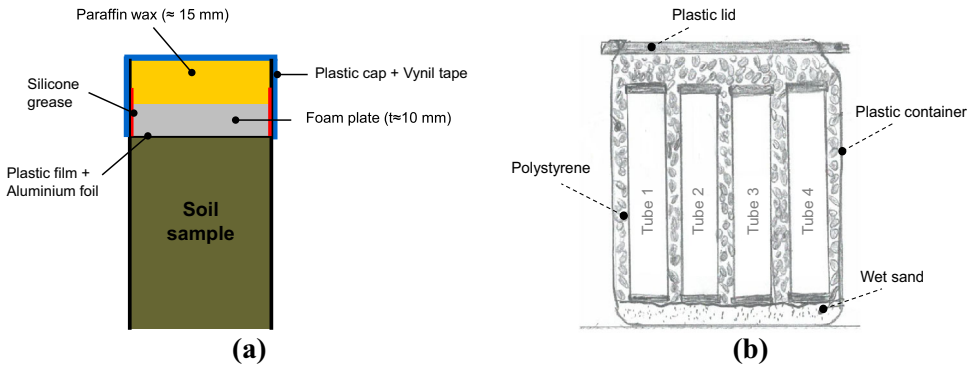

Fig. 30 Sealing and packing of tube specimens

Table 3 Methods for sample quality assessment based on ε_v and void ratio

Level	Anderson and Kolstad [1]		Lunne et al. [43]		
	ε_v (%)	Rating	$1 < OCR < 2$ $\Delta e/e_0$	$1 < OCR < 2$ $\Delta e/e_0$	Rating
1	<1	Very good to excellent	<0.04	<0.03	Very good to excellent
2	1–2	Good to fair	0.04–0.07	0.03–0.05	Good to fair
3	2–4	Poor	0.07–0.14	0.05–0.10	Poor
4	4–8	Very poor	>0.14	>0.10	Very poor
	>8				

more recently by Lunne et al. [43] have a good track record as indicators of sample quality in soft soils. These are based on recompression deformation (ε_v or $\Delta e/e_0$) to the in situ vertical effective stress. Sample quality is ranked using four levels (see Table 3): (1) very good to excellent, (2) good to fair, (3) poor, and (4) very poor. The method by Lunne et al. [43] also considers the influence of OCR and, therefore, it has become popular in the assessment of sample quality in soft soils. It is important to note, however, that these methods were developed using laboratory results obtained primarily for marine clays (PI between 6 and 43) retrieved from relatively shallow depths (<25 m). Although the influence of OCR is accounted for, no correction is considered for recompression to in situ stress in specimens subjected to large stress relief due to sampling (high overburden pressures). This issue has been recently evaluated by Krage et al. [35] using artificial silica silt–kaolin mixtures to prepare reconstituted specimens with PI ranging from 0 to 31%. Oedometer specimens were subjected to a wide range of overburden stresses ($20 < \sigma'_{v0} < 500$ kPa) to establish depositional stress history. Two levels of disturbance were then induced as follows: 1D 'perfect sampling' (1DPS) and highly disturbed (HD) state. 1D 'perfect sampling' condition was achieved via removal of deviatoric stress until reaching $K_0 = 1$, whereas highly disturbed specimens were obtained by applying a freezing–thawing cycle under unstressed conditions. HD samples were subsequently loaded beyond the preconsolidation stress, followed by unloading until achieving $K_0 = 1$, as imposed to 1DPS specimens. Finally, both 1DPS and HD samples were loaded further to a vertical effective stress of 2500 kPa. Figure 31a, b shows the compressibility curves obtained from 1DPS and HD specimens, respectively. Strong influence of the previous freezing–thawing cycle on the compressibility of HD specimens can be seen, which also affects the preconsolidation stress. Figure 31c shows the variation of the normalized void ratio ($\Delta e/e_0$) against the overburden stress obtained from 1DPS and HD specimens. The quality of HD specimens ranges from very good to excellent to poor sample quality. These results are clearly inconsistent with level of disturbance induced to each specimen and highlight the need for considering the influence of the stress relief (overburden stress) on $\Delta e/e_0$.

Classification methods described above are based on outputs from element tests which require days or weeks to get tested. It makes them unsuitable for quick assessment of sample quality. This fact has prompted interest on non-destructive sample quality examination techniques. The two most often employed in a quantitative manner appear to be those based on shear wave measurements or/and suction. However, image analysis techniques (X-Ray and CAT analysis) are becoming popular due to the recent advances in image treatments.

Image analysis

Visual inspection of the sample quality is only possible after complete soil extrusion which is not practical since the time required for visual inspection, sample selection,

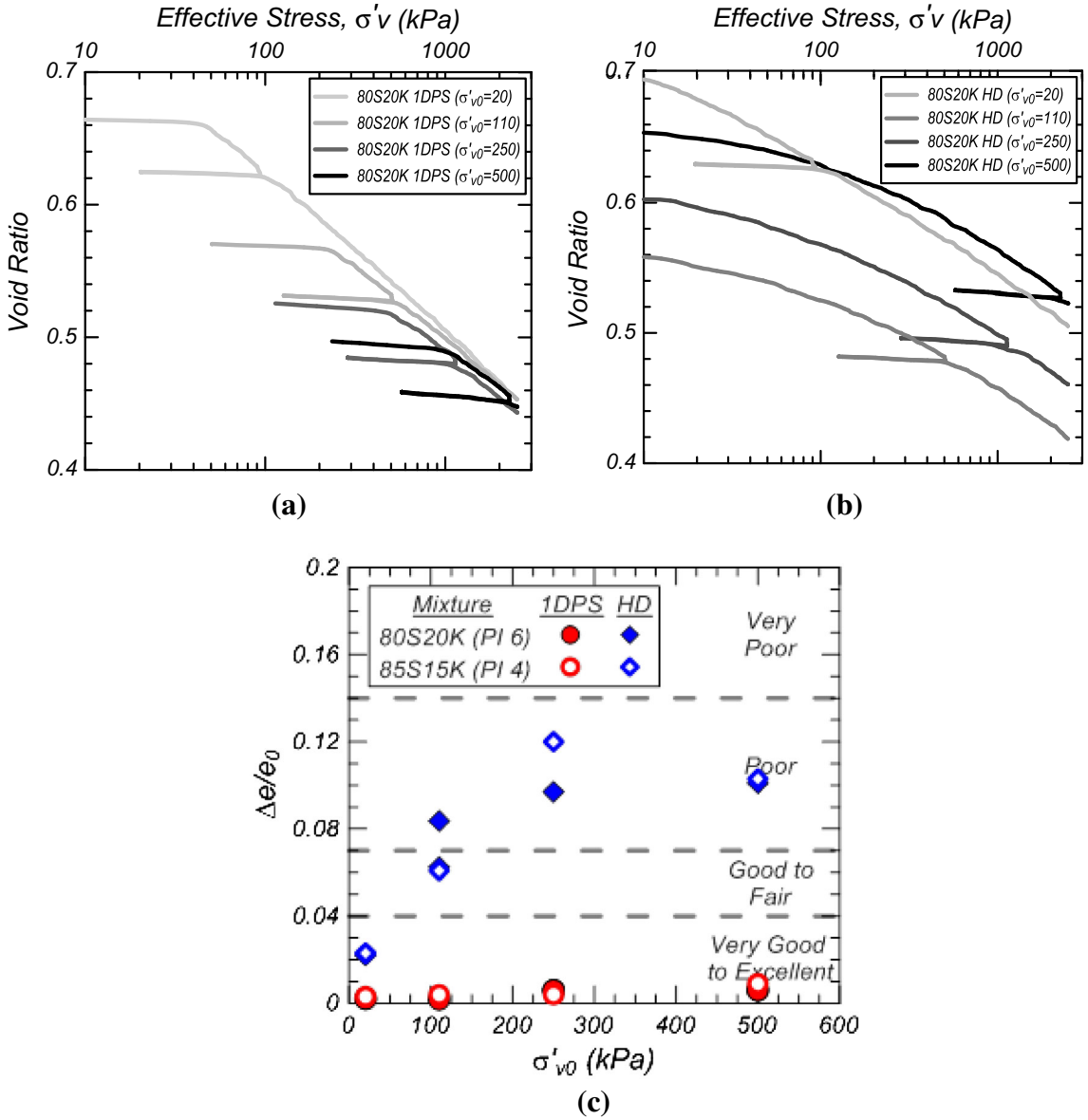

Fig. 31 Sample disturbance in low-plasticity soil. **a** Compressibility curves of 1DPS specimens. **b** Compressibility curves of HD specimens. **c** Sample quality rating for 1D perfect sampled (1DPS) and highly disturbed (HD) specimens [35]

and preparation (or sealing) is too long and may affect the initial state of the soft clay (e.g., due to moisture redistribution and drying). Non-conventional techniques like X-ray or computer axial tomography (CAT) analysis are becoming popular in geotechnical engineering due to their non-destructive nature and simple procedure. The main drawback of the X-ray technique is that all features of the specimen are superimposed into a 2D image whereas a 3D reconstruction is obtained from CAT analysis. It gives not only a 3D picture of the sedimentary structures but also natural heterogeneities (fissures, inclusions, cavities) and allows selection of high-quality specimens for laboratory testing. CAT imaging is based on Beer's law that relates the incident intensity (I_0) and transmitted intensity (I) of a X-ray or gamma-ray beam passing over an entire transverse section by means of a linear attenuation coefficient (μ) (e.g., [16]):

$$I = I_0 \exp(-\mu \cdot x) \tag{4}$$

where x is the sample width. The imaging process can be summarized as follows. The specimen is placed on a table whose movement can be accurately controlled. An X-ray source generates a continuous beam of X-rays that passes through the object impacting the detector. The rotation of the source and detectors (gantry) determines a virtual section through the sample ('slice'). As result of the

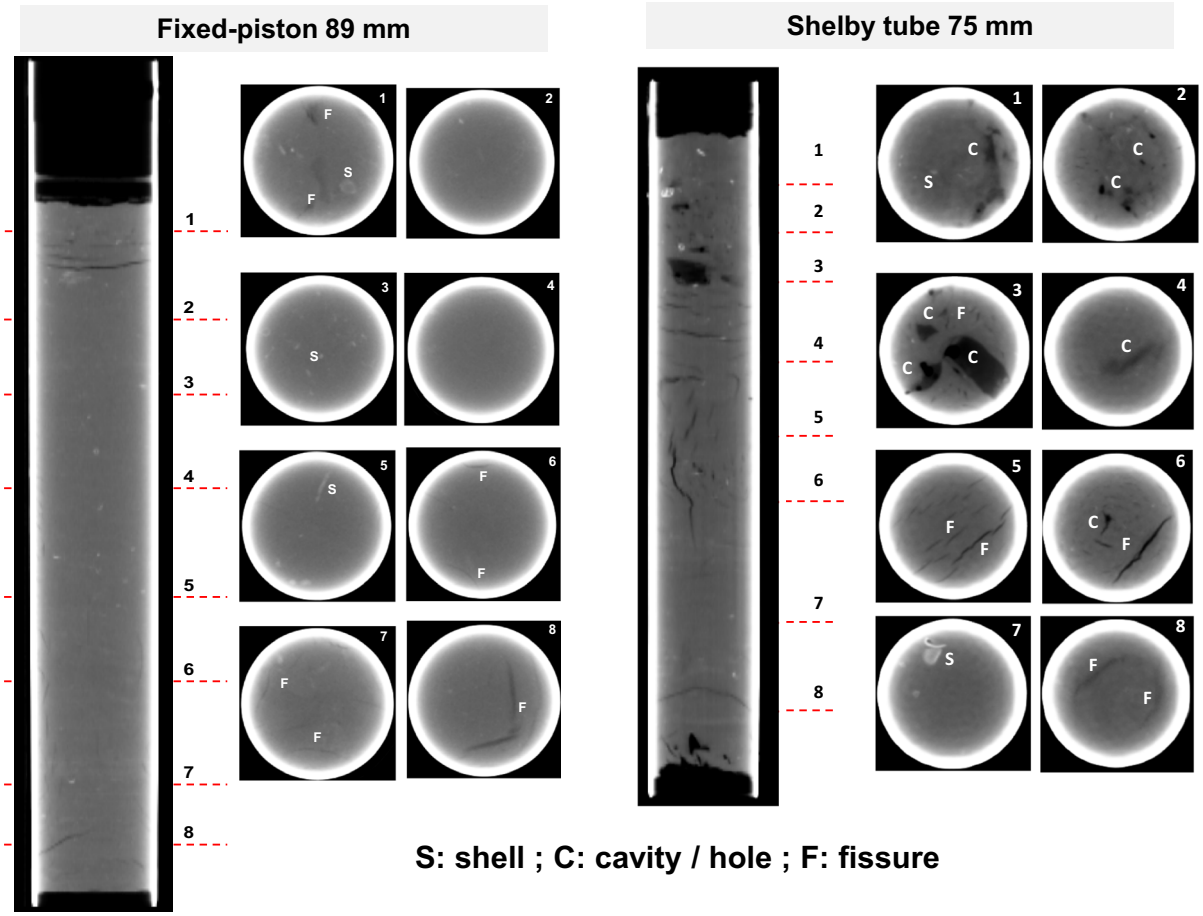

Fig. 32 Qualitative CAT analysis in Ballina clay (Australia)

reconstruction algorithm, this virtual section is decomposed into prismatic volumetric elements or voxels (typically 512 × 512 in medical instruments). The height of the voxel is equal to the slice width of the X-ray beam. Each voxel is assigned an average value of the linear attenuation coefficient, μ, expressed in Hounsfield units or CT values. For imaging, these values are proportionally scaled into shades of gray. The set of slices from the scanned object is named stack.

The maximum energy of medical X-ray CT scanners ranges between 120 and 140 keV. These devices are designed for use on human subjects to image soft tissue and bones. Human bones have similar density as natural soft soils (<2 mg/m^3) and, therefore, it might be reasonable to use them on soft soil deposits. Equation (4) implies that for given density and incident intensity (I_0), an increase of sample width will decrease the transmitted signal (I). In other words, increasing of the sample width will decrease the quality of the scans. Although it would (a priori) reduce the use of X-ray scanners to small-diameter samples (i.e., tube specimens), it will be demonstrated below that reliable results can be obtained on large-diameter block specimens using further image treatments.

Computer axial tomography analysis is nowadays common practice at the University of Newcastle (Australia) to examine qualitatively the internal structure of soft soil tube samples. Figure 32 shows the vertical sections of two tube specimens, retrieved from two near-by boreholes at the Ballina field testing facility [34] using an Osterberg fixed piston sampler (Fig. 32a) and a Shelby tube (Fig. 32b). Both tube specimens were retrieved from a depth of 7.5–8.1 m. The fixed piston sampler has an outer diameter of 89 mm, 5° cutting edge and area ratio equal to 9%. The U75 (Shelby), commonly used in Australian practice, has an outer diameter of 75 mm and an area ratio of 8%. The cutting edge is 15 degrees. The inside clearance ratio is zero in both cases. CAT analysis was carried out using 130 keV maximum energy and 178 mA intensity. Particular emphasis was made here on the detection of possible heterogeneities and their potential influence on laboratory testing. In this qualitative analysis, the free software Gimias® [23] was employed for image post-processing. The attenuation scale shown in Fig. 32 varies from white (maximum attenuation or high material density) to black (minimum attenuation or low density).

The comparison of the vertical sections clearly shows important differences between tubes as a consequence of sample disturbance. The specimen retrieved with the fixed piston sampler seems quite homogeneous with a few sub-horizontal cracks observed at top and bottom ends. A highly disturbed specimen was obtained with the Shelby tube. Sub-horizontal cracks as well as vertical fissures and cavities are clearly identified along the 75-mm Shelby tube (Fig. 32b). Figure 32 also shows cross-sectional images at different depths along the tubes. Here, capital letters F, C and S stand, respectively, for fissure/heterogeneity, cavity/channel, and shell. The presence of fissures cavities and shells can be noted in the Shelby tube, which makes it difficult to obtain representative specimens for laboratory testing (i.e., oedometer and triaxial tests). The black hole located at the top of the tube represents a cavity which is assumed to be induced during sampling. In the specimen retrieved with the fixed-piston sampler, the inspection of Fig. 32 suggests that soil from slice 2–7 could be used for laboratory testing whereas top and bottom ends should be employed only for characterization purposes as suggested by Ladd and DeGroot [37]. Overall, CT images indicate that open sampler U75 induces higher soil disturbance than fixed piston samplers despite its lower area ratio.

Quantitative CAT analysis provides an opportunity to obtain density maps of scanned samples. This is a valuable outcome for practitioners as it would reduce the uncertainty associated with the selection of soil specimens for laboratory testing. Two extra steps are required to obtain density maps due to the influence of several artifacts that made difficult the interpretation of the resulting images. On the one hand, a quantitative relationship between attenuation coefficient and bulk density has to be established. The relationship between X-ray attenuation and bulk density is strongly soil dependent as it is affected by porosity, water content, and chemical composition. Empirical correlations are frequently employed (e.g., [2, 53]). On the other hand, artifacts such as background noise, rings, and outliners have to be detected and treated as they impact on CT numbers and, therefore, on density estimations.

An interesting example has been recently reported by Sau et al. [63] who use CAT to obtain density maps in 250 mm in diameter block (Sherbrooke) specimens of silty clay deposits from Castelló d'Empuries (Spain), previously described in this paper. In line with the decrease in image quality with the sample diameter, the analysis of block specimens is clearly more demanding. A medical X-ray CT scanner (Siemens Somaton Spirit® scanner) was used to acquire the CT images. Samples were scanned with X-ray tube voltage of 130 kV and 178 mA tube current. Radiographic exposure was 122 mA s and 411 mm field of reconstruction was captured in a 512×512 pixel image. 194 contiguous two-dimensional 12-bit CT images, spaced every 5 mm, were acquired. The in-plane resolution obtained was 0.8×0.8 mm^2/pixel and the slice thickness 5 mm. The calibration curve between X-ray attenuation and bulk density determined by Sau [62] was used to analyze the CT scans of the Sherbrooke specimens. The main artifacts affecting the scans of the Sherbrooke specimens were high background noise and ring artifacts. An example of ring artifacts is shown in Fig. 33a. They appear on CT images as a number of dark concentric rings of one pixel width superimposed on the structures being scanned. It is impossible to separately remove this artifact due to the large amount of background noise of the images. Background noise is the local statistical fluctuation in the gray values of individual picture elements within a homogeneous region. Noisy CT images are characterized by a grainy appearance of the image which results from pixels with extreme attenuation values (outliers). Figure 33b shows a typical example of the background noise obtained in a slice from a Sherbrooke specimen. Noise and ring artifacts were not separately removed, but the filters used to remove noise did also remove dark pixels from the rings.

The free software ImageJ was used for image post-processing. A rank-median filter was applied. This filter replaces each pixel outlier value with a median of neighboring pixel values. The following parameters were required to apply the rank-median filter [63]:

- Radius: determines the neighboring area (in pixels) used for calculating the median.
- Threshold: defines by how much the pixel must deviate from the median to get replaced.
- Outliers selection: determines whether pixels brighter or darker than the surrounding (the median) should be replaced.

The inspection of the block CT scans showed that the amount of noise was not uniform. There was more noise in the center, whereas the periphery was far less noisy. The

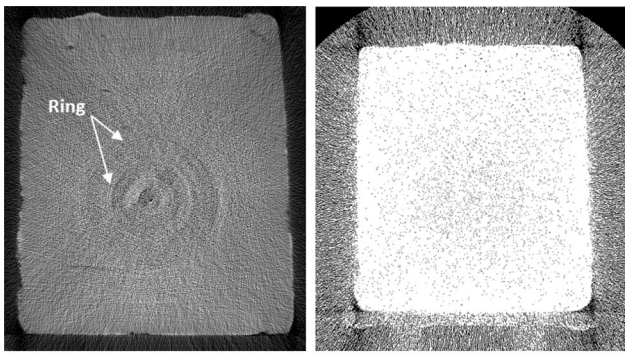

Fig. 33 Ring artifact and background noise in Sherbrooke specimens [63]

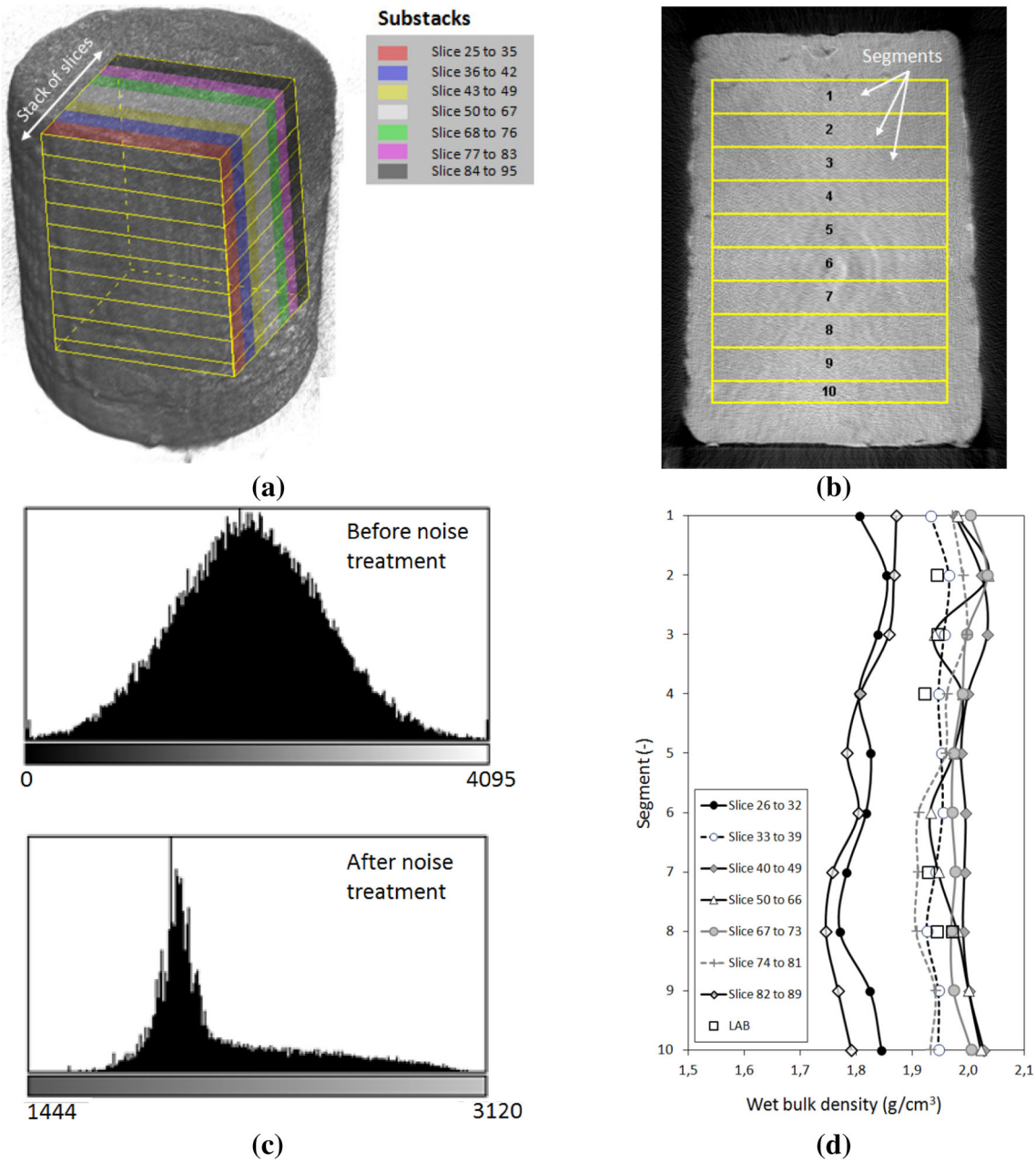

Fig. 34 **a** 3D reconstruction of Sherbrooke specimens with substacks. **b** Slice with defined region of interest. **c** Histograms of *gray* values before and after noise treatment. **d** Computed and laboratory estimates of bulk density for Sherbcfarooke specimen [63]

amount of noise varied from top to bottom of the block. Good results were obtained using substacks, i.e., set of slices grouped according to the level of noise, and, for each substack, define different regions of interest (ROIs), here named segments. The filter process was independently applied to each of the segments.

Figure 34a shows a 3D reconstruction of a Sherbrooke sample, illustrating the substacks and segments created. Figure 34b further clarifies the definition of the segments. These segments are the same in all slices. The median-based filter is applied several times sequentially. In this case, the iteration ended when the minimum and maximum gray values were about 1800 and 3100, respectively. This range defines minimum and maximum gray values adopted by Sau et al. [63] as exclusion criteria to define the outliers. Therefore, gray values lower or higher than 1800 and 3100, respectively, were considered outliers. Histograms before and after noise treatment are shown in Fig. 34c. Additional details are given by Sau [62] and Sau et al. [63].

After noise removal, a density profile was obtained for each substack of slices. Figure 34d shows the density profiles of substacks of a Sherbrooke sample. These values

are compared against laboratory measurements obtained from oedometer and triaxial specimens. Results from the imaging process indicate that the block sample is homogeneous, except at its periphery where lower values are detected. This is attributed to the disturbance caused by sampling. Good agreement is observed between laboratory data and the density inferred from the block CT scan. A similar approach has been used by Sau [62] to obtain density maps in tube specimens, where noise and ring artifacts are less significant. The results described above highlight the capabilities of not only qualitative but also quantitative CAT analysis for assessing sample quality in soft soils.

Suction measurements

Soil suction was first suggested as an indicator of sampling disturbance by Ladd and Lambe [36], using the so-called "perfect sample" effective stress, σ'_{ps} as a reference. That is the isotropic effective stress value remaining after undrained unloading of the deviatoric "in situ" stress. Such value is not usually known in advance and is not simple to estimate, because it requires knowledge of K_0 and the Skempton's A parameter. To overcome this issue, the approach followed in practice uses the in situ vertical effective stress to normalize the measured suction (u_r/σ'_{v0}).

Figure 35a shows measurements reported by Donohue and Long [15] for three natural soils of low plasticity: Bogganfin, Ballinasloe (Ireland), and Onsoy (Norway). There is a clear trend between normalized suction (u_r/σ'_{v0}) and sample quality descriptor $\Delta e/e_0$. The highest values of normalized suction are provided by Sherbrooke specimens whereas open drive samplers provide the lowest measures. Donahue and Long [15] reported a suction around $0.2\sigma'_{v0}$ for $\Delta e/e_0 = 0$ which is similar to the value suggested by [70] for undisturbed soft clays. Sometimes suction does not show clear trends with sample quality. This is the case of the silty clays from Castelló d'Empuries [3]. As shown in Fig. 35b, the Shelby tube provides a suction value above $0.40\ \sigma'_{v0}$, at least for times higher than the value measured in the fixed piston. Most measurements indicate very small residual stress values. There is no relationship between the normalized suction ratio value and sample quality for these silty deposits. These results are in agreement with the observations reported given by Tanaka [70]. He showed that u_r is strongly controlled by OCR and other factors such as clay content, plasticity index, and soil permeability. Therefore, correlations based on u_r appear to be highly site specific and sometimes no overall trend is generally discerned.

Shear wave velocity measurements

One of the most common non-destructive techniques to assess sample quality is the estimation of the shear wave velocity (or small-strain shear modulus) via wave propagation methods such as bender elements [17] or shear plates (e.g., [30]). Shear waves are preferred against compressional waves as they can only propagate through the soil skeleton and, therefore, they provide useful information about changes in soil fabric, as those caused by sampling. Laboratory measurements are conveniently normalized against in situ values (e.g., CPTu, SDMT) to have an estimation of the reduction in soil stiffness due to

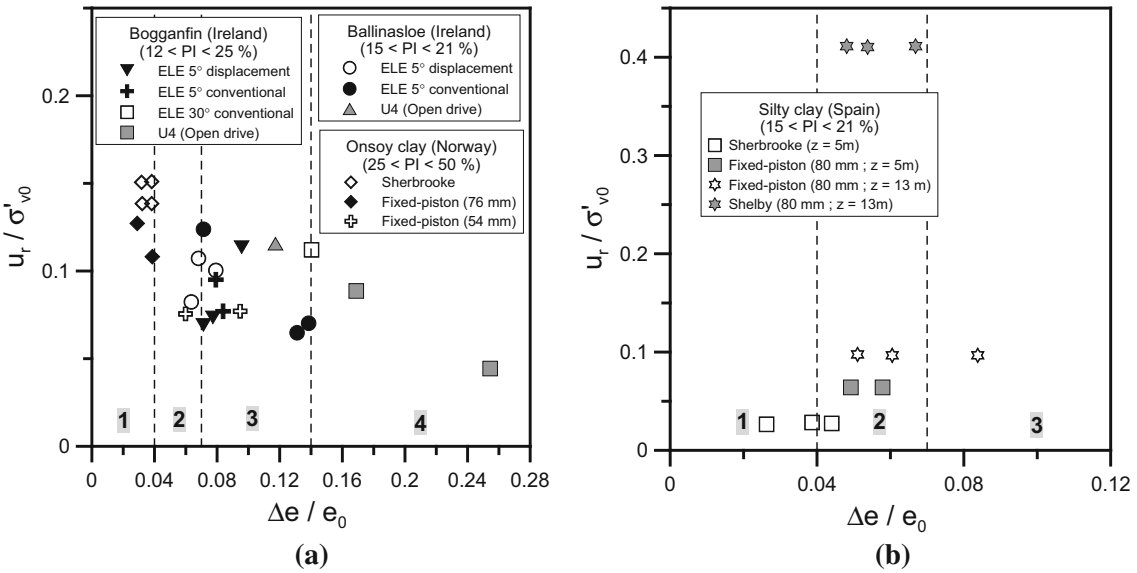

Fig. 35 Normalized suction vs Lunne's et al. sample quality indicator. **a** Bogganfin, Ballinasloe, and Onsoy clay [15]. **b** Silty deposits from Castelló d'Empuries [3]

sampling. Values of shear wave velocity measured at unconfined conditions (e.g., [15, 38]) as well as at in situ stress conditions (e.g., [68, 69]) are the two procedures followed in laboratory to assess sample quality using wave propagation techniques. Both have shown good correlation with sample quality descriptors ε_v and $\Delta e/e_0$ for a wide variety of soils. Figure 36 shows V_s estimates for three natural soils: low-plasticity Boston Blue clay (USA) [38], low-plasticity silty deposits from Castelló d'Empuries [3] as well as high-plasticity Ballina clay [58]. Block (Sherbrooke) specimens as well as tube samples (fixed piston, Shelby tube, and SPT samplers) are included in this figure. Good correlation between normalized shear wave velocity ($V_{s\text{-}(BE)}/V_{s\text{-}(SDMT)}$) and sample quality ($\Delta e/e_0$) is observed. Results shown in Fig. 36a correspond to V_s estimates after recompression to the in situ vertical effective stress in CRS tests values obtained at unconfined conditions are shown in Fig. 36b. Sherbrooke specimens provide the lowest reduction in shear wave velocity followed by fixed piston samplers and Shelby tubes. Recompression to the in situ stress in high-plasticity Ballina clay provides values of V_s close to the in situ measures. In the case of the low-plasticity silty deposits, recompression increased V_s to $0.80V_{s\text{-}(SMDT)}$ for $\Delta e/e_0 = 0$. Arroyo et al. [3] observed that the normalized shear wave measurements showed a better correlation with sample quality when taken after recompression than when taken after re-saturation. Values reported by Landon et al. [38] for Boston Blue Clay show a clear ordering of V_s with sample quality, with the Sherbrooke rating above the piston tubes, those above the Shelby and STP. V_s reduced to $0.35V_{s\text{-}(SDMT)}$ and $0.15\ V_{s\text{-}(SDMT)}$ in specimens retrieved with Shelby tube and SPT sampler, respectively.

Despite the simplicity and cost-effective nature of the shear wave propagation technique as a tool to assess sample quality, it is important to recognize the fact that sampling may affect the soil stiffness in two opposite ways. On the one hand, soil stiffness may decrease due to soil destructuration. On the other hand, it may increase if soil destructuration causes a reduction in porosity (soil compression). These two effects may cancel each other and mask the true influence of sampling on soil fabric. It is thus difficult to establish a priori the nature of the change that sampling will induce.

Microstructural analysis

Although microstructural techniques such as scanning electron microscope (SEM and ESEM), micro-tomography (μ-CT scanning) and mercury intrusion porosimetry (MIP) are not commonly employed in practice to evaluate changes in soil fabric due to sampling, they offer vital information to identify microstructural changes which in turn affects the macroscopic mechanical behavior of natural soils. Despite its obvious relevance, the changes in the soil microstructure that occurs during tube sampling do not appear to have been evaluated directly in previous literature.

A comprehensive experimental investigation aimed to evaluate the microstructural modifications caused by tube sampling in Ballina clay has been recently reported by Pineda et al. [59]. Attention was focused on evaluating differences in soil microstructure, in terms of the pore size

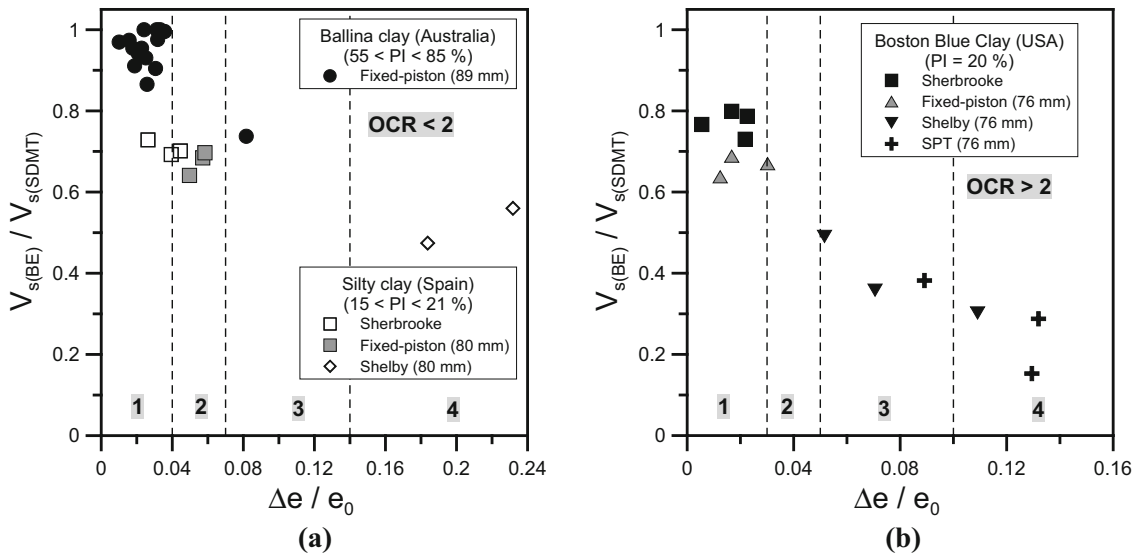

Fig. 36 Normalized shear wave velocity vs Lunne's et al. sample quality indicator. **a** Ballina clay [58] and silty deposits [3]. **b** Boston Blue Clay [38]

distribution estimated from MIP tests, for specimens located at different levels along the centreline and the perimeter within the tube. Three tube specimens were tested. They were retrieved at the Ballina field testing facility [34] from three boreholes at depths between 7.5 and 8.2 m. Two open (Shelby) samplers (external diameter B of 50 and 75 mm) were used in boreholes Mex 1 and VPW 1, respectively. A hydraulic, Osterberg-type, fixed piston sampler ($B = 89$ mm) was employed in borehole Mex 9.

The sampler types were selected to include the most common ones used in practice (Shelby tubes) as well as the 'most adequate' (fixed piston) sampler commercially available for soft soils. The samplers have ratios B/t (external diameter to wall thickness) ranging between 31 and 49 (Table 4). The 50-mm Shelby tube has a B/t ratio of less than 40 and, therefore, disturbance should be expected [37]. On the other hand, the 75-mm Shelby tube has the largest B/t ratio (49) which, a priori, would provide good quality tube specimens. Block specimens of natural clay were also obtained at Ballina site using the Sherbrooke sampler to provide information about the undisturbed material. The Sherbrooke specimen was obtained from borehole BH1 at depths between 7.4 and 7.9 m.

For soils that display an interconnected porosity, the mercury intrusion porosimetry (MIP) technique is commonly employed to infer the pore size distribution (PSD) which provides information about the fabric of the soil mass (e.g., [13]). Therefore, changes in the soil fabric caused by tube sampling would be reflected in the PSD curve. The principle of MIP is based on the Washburn equation [82], which relates the applied mercury injection pressure p to an equivalent entrance pore size d, as described by the following equation:

$$p = \frac{-4\sigma_{Hg}\cos\theta_{nw}}{d} \tag{5}$$

where σ_{Hg} is the surface tension of mercury (0.484 N/m at 25 °C, as adopted by Diamond [12], Delage and Lefebvre [13]) and σ_{nw} is the mercury–soil contact angle (assumed equal to 140° as adopted by Romero [61]). Values of the void ratio associated with intruded mercury are computed from the test results obtained during the intrusion stage as $e_{MIP} = V_{mercury}/V_{solids}$, where V_{solids} is the volume of the dry solids used for the MIP test and $V_{mercury}$ is the cumulative volume of intruded mercury at the current pressure. The pore size density function is estimated from the derivative of the cumulative intrusion curve according to:

$$f(\log x_m) = \frac{\delta(e_{MIP})}{\delta(\log d)} \tag{6}$$

where $\log(x_m)$ is the midpoint of the pore diameter class.

Prior to soil extrusion, the specimens were scanned using computerized axial tomography (CAT) to conduct a qualitative assessment of the tube quality. Based on the CAT images, five levels per tube (A–E) were selected to trim specimens for MIP testing (Fig. 37). Levels A and E correspond to soil samples trimmed close to the top and bottom ends, specifically within a zone of $z < B$. Levels B and D refer to soil located between $B < z < 1.5\ B$, i.e., at the boundary of the disturbed zone described in Ladd and De Groot [37] which should be avoided for mechanical testing. Level C corresponds to the middle part of the specimen. Small sub-samples (≈ 125 mm^3) were trimmed from the centerline and perimeter using a thin wire saw as shown in Fig. 18. Specimens were subjected to freeze-drying prior MIP testing as recommended by Delage and Lefebvre [12]. Additional details are given in Pineda et al [59].

The modifications in soil fabric were evaluated by comparing the MIP results obtained from tube specimens against the PSD curves of the Sherbrooke specimens

Table 4 Characteristics of the tube samplers

Sampler type	B/t, (–)	α, (°)	AR, (%)	ICR, (%)
50-mm Shelby	31	12	14	0
75-mm Shelby	49	15	9	0
89-mm fixed piston	45	13	10	0

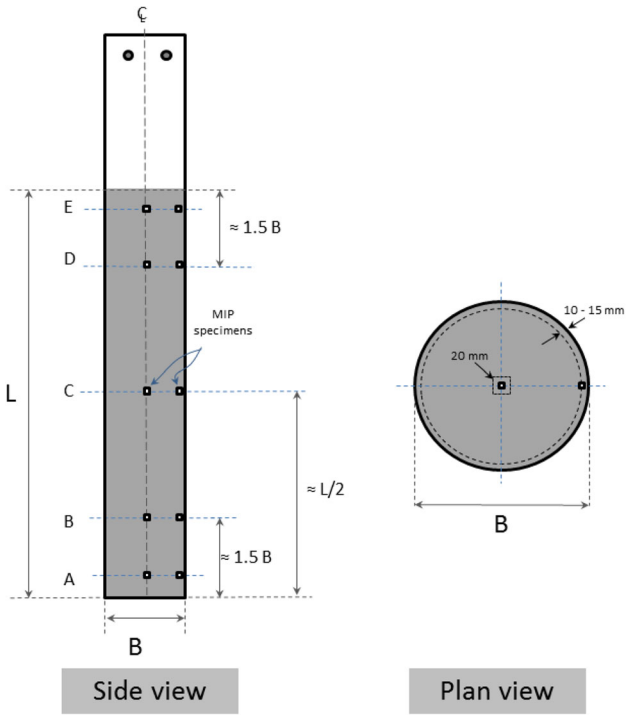

Fig. 37 Schematic location of MIP specimens within the tube sampler

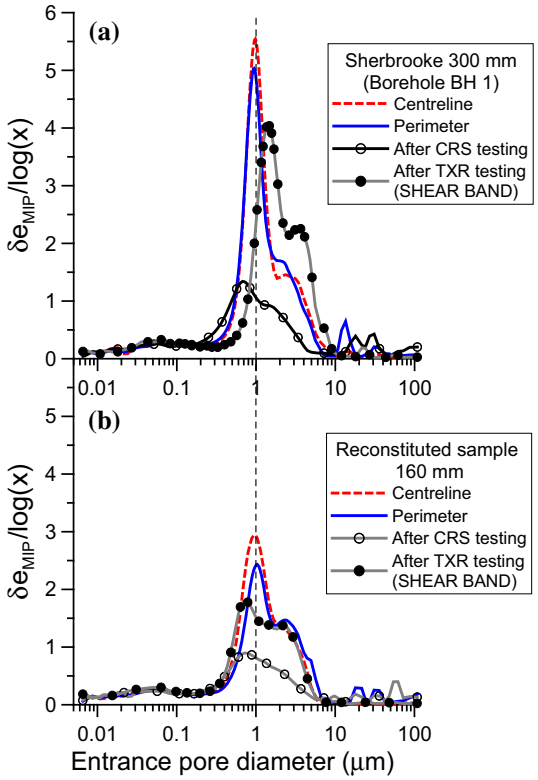

Fig. 38 PSD curves. **a** Sherbrooke (undisturbed) specimens. **b** Reconstituted specimens

(undisturbed clay). The PSD curves for specimens trimmed from the Sherbrooke sample are shown in Fig. 19a. This is complemented with the MIP results for reconstituted clay using specimens trimmed from the perimeter and centreline of a 160-mm sample (Fig. 38b). The comparison of the PSD curves shows a similar dominant pore size of around 1 μm for both the Sherbrooke and the reconstituted clay, whereas the peak density values for the former are significantly higher. These results suggest that both the natural and the reconstituted clay have a similar structural arrangement, but the former has larger numbers of pores with dominant size. Thus, the reconstitution process seems to produce a similar fabric, while erasing a significant proportion of pores with the dominant size.

These similarities in soil fabric are clearly observed in Fig. 39 where microscope images obtained from scanning electron microscope (SEM) analysis, for the natural and the reconstituted clay, are presented. The SEM analysis was carried out on specimens previously subjected to the freeze-drying process. The predominance of macropores of around 1 μm for the natural and the reconstituted clay is confirmed at large magnification, which supports the results from the MIP analysis. Both natural and reconstituted clay show an open fabric, although this is clearer for the natural clay. A clear pattern of fabric anisotropy is not evident for the natural Ballina clay. This feature is in agreement with the non-oriented fabric described by Mitchell [47] for soft marine illitic clays.

Figure 38 also includes the PSDs for natural and reconstituted specimens subjected to two different mechanical tests prior to MIP testing: (i) one-dimensional loading under constant rate of strain (CRS) conditions (empty circles) and (ii) CK0U triaxial testing (filled circles). In the latter case, MIP specimens were trimmed from the failure zone (shear band) where shear strains concentrate.

The 1-D loading slightly reduces the dominant pore size and its corresponding peak density. However, the pores with entrance diameters below 0.2 μm (Sherbrooke) and 0.5 μm (reconstituted) remain almost unchanged. This suggests that 1-D loading erases large numbers of pores

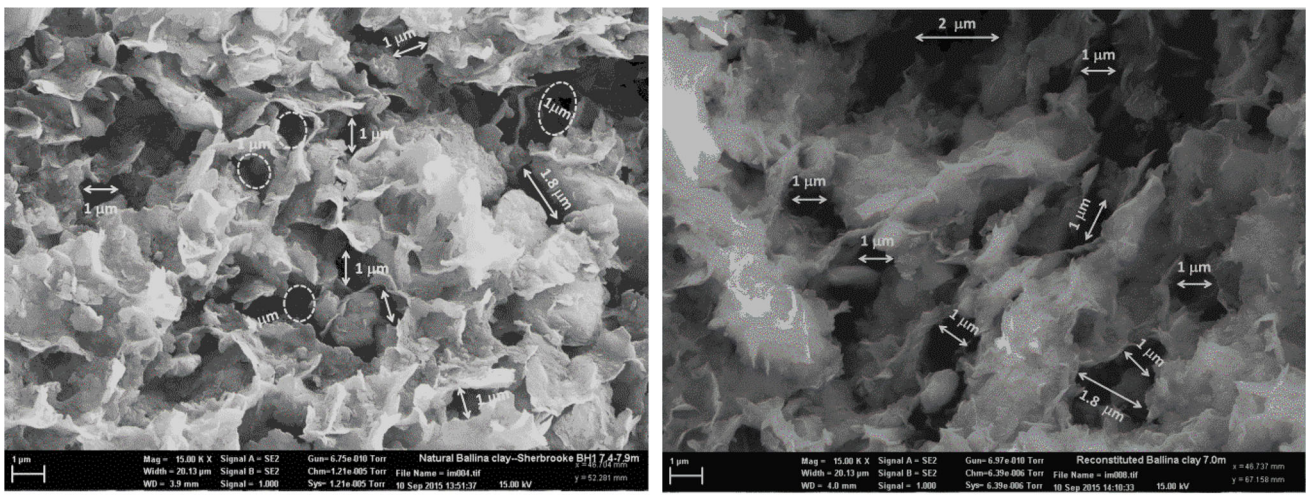

Fig. 39 SEM images (×15,000). **a** Sherbrooke (undisturbed) specimen. (b) Reconstituted specimen

having entrance diameters between 1 and 6 μm, but does not affect these pores below 0.2 and 0.5 μm, respectively. Regarding the samples trimmed from the shear band, two different responses are observed. For the natural (Sherbrooke) specimen, undrained shearing increases the dominant pore size up to 1.7 μm, reduces the peak density and shifts the PSD towards large pore diameters. On the other hand, the reconstituted specimen shows a reduction in the dominant pore diameter and peak density without important shifting of the PSD. This response is similar to the PSD of specimens previously subjected to CRS loading, in which compression is dominant.

The spatial variation of void ratio and water content within the 50-, 75-mm Shelby tubes as well as the 89-mm fixed piston sampler is shown in Figs. 40a, 41a, and 42a, respectively. Values of void ratio obtained from MIP specimens as well as estimations of water content and void ratio from specimens trimmed for triaxial and oedometer testing are included in these figures. In general, lower void ratios are measured at the bottom half of the tubes with the natural water content lying around 108.5–112%. Void ratio increases up to 3.17 at the upper end which is consistent with the increase in water content (up to 119%). This behavior is more pronounced in the Shelby tubes. The 89-mm fixed piston shows more symmetric variation between upper and bottom halves, which indicates the

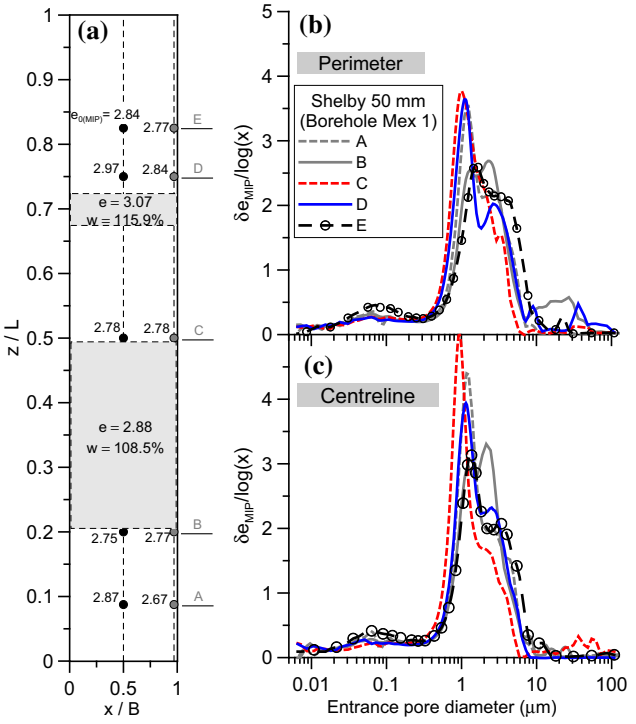

Fig. 40 Water content (void ratio) variation and PSD *curves* for specimens from the 50-mm Shelby

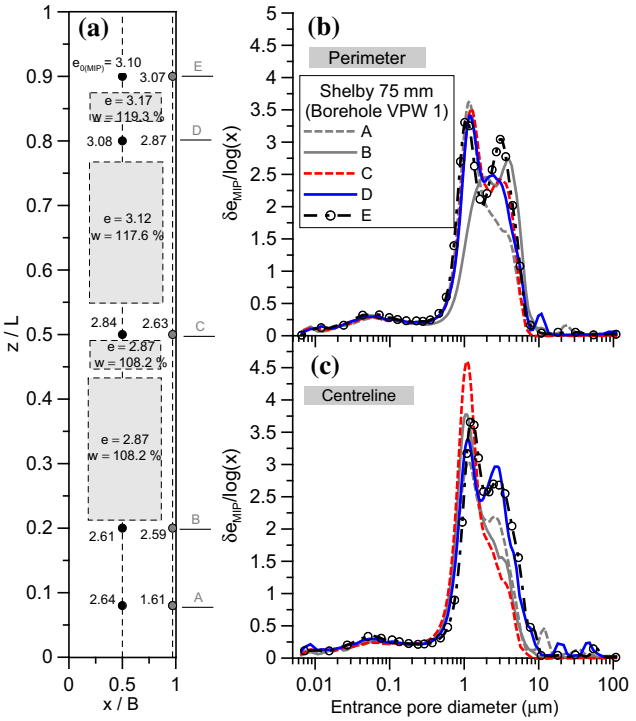

Fig. 41 Water content (void ratio) variation and PSD *curves* for specimens from the 75-mm Shelby

beneficial effect in using the piston. From the inspection of the PSD curves shown in Figs. 40b, c, 41b, c, and 42b, c the following aspects may be remarked:

- A predominant mono-modal PSD is observed in all cases.
- The PSD shows important differences along each tube. This behavior is more evident in Shelby tubes.
- The dominant pore size for specimens located at the top and bottom ends increases whereas their corresponding peak density values as well as the PSD shifts towards the right (larger pore diameters).
- The PSD curves for specimens from the 89-mm fixed piston are more symmetric than those from the perimeter. It indicates lower levels of change to the structure of the natural clay.

Figure 43 compares the PSD curves for the three tube samplers used in this study for levels A (bottom end), C (middle), and E (top end). The PSD for the centreline of the Sherbrooke specimen is also included in these figures as a reference. Larger microstructural modifications are produced by the Shelby tubes near the perimeter of the sampler (Fig. 43a). This leads to the creation of new macropores as indicated by appearance of secondary peaks in the PSDs. The 89-mm fixed piston sampler also affects the PSD. The top end of the specimen (level E) seems to be more sensitive to tube sampling, although some changes in

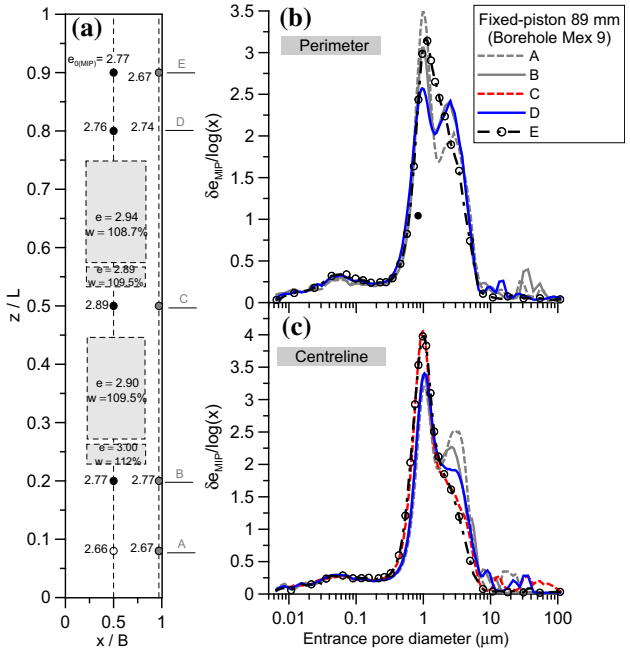

Fig. 42 Water content (void ratio) variation and PSD *curves* for specimens from the 89-mm fixed piston

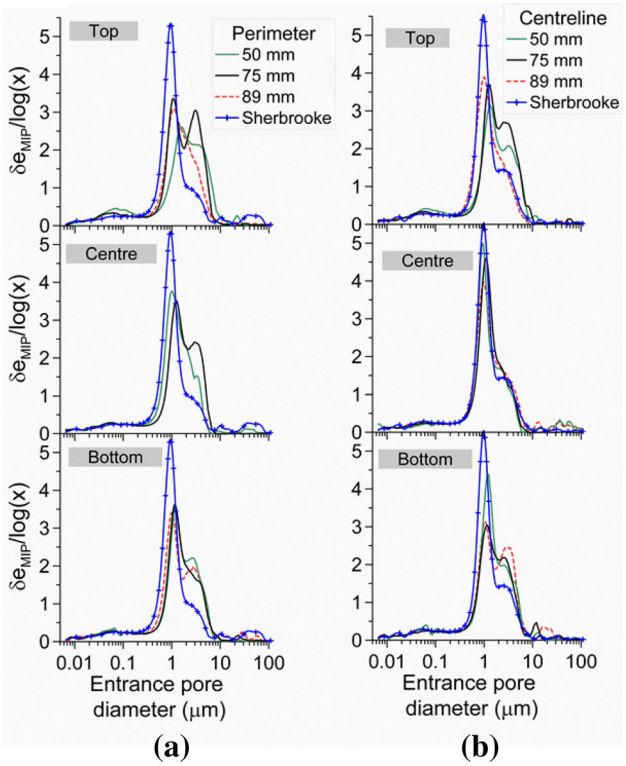

Fig. 43 Influence of the sampler type on the PSD at levels A, C, and E

the PSD are detected even at level C. Variations in the PSD are also detected along the centreline of the sampler (Fig. 43b). Again, the Shelby tubes produce new macropores and affect the shape of the PSD at levels E and A. The 89-mm fixed piston tube also seems to cause changes in the PSD. On the other hand, almost identical PSD curves are observed in the specimens located at level C which is in agreement with the similar void ratio estimated for all the specimens tested (see Figs. 40a, 41a, and 42a).

A small reduction in the peak density value and a minimal increase in the dominant pore size are observed at this level. This clearly suggests that soil which is sampled close to the middle of the tube is less affected by the sampling process. It was shown that (1) the decreasing peak in the PSD indicates a reduction in the number of pores with the dominant size (e.g., by compression), (2) even slight increases in the dominant pore size indicates an enhancement of the macro porosity, and (3) the appearance of new (secondary) peaks in the PSD at large entrance pore sizes is associated with the creation of macro porosity. At level C on the centreline, only mechanisms 1 and 2 are significant, suggesting that axial deformation is the main consequence of tube sampling.

The comparison against the PSD from specimens subjected to CRS loading (see Fig. 38) supports this conclusion. The appearance of new peaks at the top and bottom ends on the centreline seems to suggest a more complex deformation mechanism that also occurs in specimens located at the perimeter of the sampler. Here, mechanisms 1, 2, and 3 are all relevant and produce similar PSD curves as the one observed for the natural specimen trimmed from the shear band after undrained shearing (see Fig. 38).

The effects of the changes in soil fabric on the mechanical behavior of Ballina clay are highlighted in Fig. 44. The stress paths followed for triaxial specimens (50 × 100 mm) trimmed from the tubes tested in this research during K_0 triaxial recompression to the in situ stress state are presented. The strong influence of the type of sampler on the volumetric compression experienced by the triaxial specimens can be seen clearly. The Sherbrooke specimen reached a maximum compression of around 3.5%. A little higher volumetric strain was measured in the specimen trimmed from the 89-mm fixed piston sampler, whereas the largest compression was observed in the specimen trimmed from the 50-mm Shelby tube ($\approx$5.5%). This behavior is in agreement with the structural modifications observed from MIP testing. Larger deformation should be expected if new macroporosity is created during tube sampling. Moreover, large volumetric strain will occur during recompression if the highly disturbed outer zone, located near the perimeter of the tube specimen, is not removed prior to triaxial testing, as occurred in the case of the 50-mm Shelby tube.

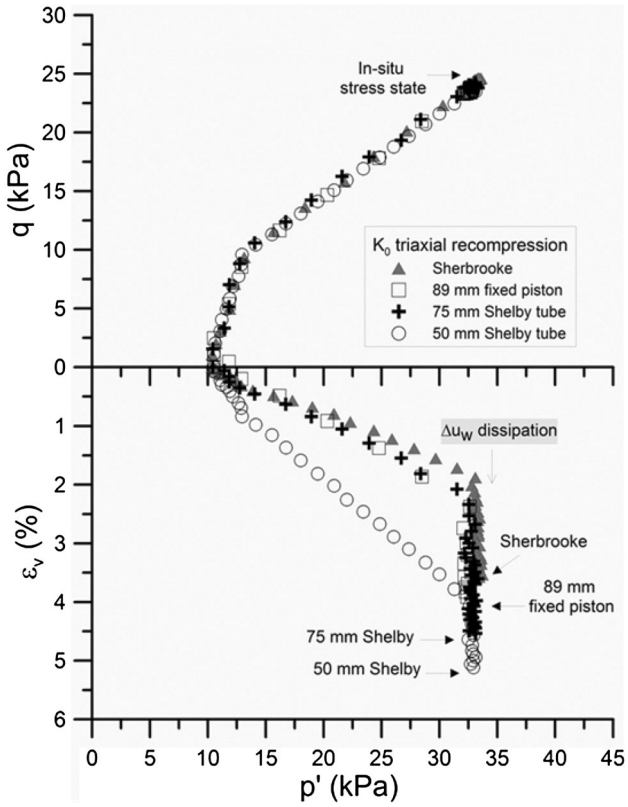

Fig. 44 Volumetric strains during K_0 triaxial recompression

Concluding remarks

In this keynote address the authors had the intention to give an insight into how can laboratory tests over representative soil samples can be considered reference methods, if some ameliorations are incorporated, relocating them in the front line of ground property characterization. This was done at three levels: sampling quality, careful reconditioning and preparation of specimens to guarantee the operational states, and integrated measuring instrumentation that can give a complete view of the soil specimen behavior using precise local strain systems that measure spatially those strains in a continuous manner.

At the level of the sampling quality, new equipments and techniques have improved the capacity of retrieving very good undisturbed samples a lot, with emphasis on the recent Gel-Push sampler with an utmost successful performance in sandy and other difficult granular soils under water table (such as silty soils in tailing ponds), by one side, and high-precision sample quality evaluation when recurring to shear wave velocities measured in situ and in lab on specimens after sampling and/or their preparation prior testing, by the other side. These steps ahead become crucial to capture and replicate the mechanical behavior of the undisturbed soil.

Soft soils are frequently encountered in civil projects around the world. There is a high degree of uncertainty about the effect of sampling disturbance as the guidelines chiefly focus on the selection of the type of sampler. Three natural soft soil deposits were used in this paper to highlight some important aspects of the sampling process as well as the sample quality assessment in soft soils. Every single stage of the sampling process plays a role on the potential disturbance of soft soils. Despite valuable experimental evidence and theoretical work being published during last decades, a unified framework for assessing sampling disturbance in soft soils is still not available. The complex hydro-geological environments in which soft soils are formed makes it difficult to develop simple and reliable tools to assess (quantitatively) the consequences of tube sampling on the mechanical parameters for different types of soft soil deposits. Several techniques, based on macroscopic measures (element tests), have been proposed to assess the representativeness of the test result. Some of them (e.g., suction measurements) are strongly site dependent. Extra care is needed when using available sample quality descriptors in low-plasticity soils subjected to large overburden stress as misleading results may be obtained. Further investigation in this regard is needed.

The advances in imaging techniques provide new tools to evaluate the modifications in soil fabric in an easy and non-expensive way. Quantitative image analysis seems a promising tool that could simplify the time-consuming (a posteriori) approach currently followed in practice to assess sample quality. The use of microstructural techniques is crucial for proper understanding of the mechanism affecting the soil fabric during sampling. It was demonstrated that important changes in soil fabric occur as a consequence of tube sampling. The type of sampler has a major influence on the structural disturbance experienced by the clay specimen. The PSD curve seems to be affected in two ways. On the one hand, at the centreline of the tube, the peak value of the PSD curve reduces. This reduction is more pronounced in small-diameter samplers and is greatest for specimens located at the top and the bottom ends of the sampler. A slight increase in the dominant pore size diameter is observed. On the other hand, a combined mechanism of reduction in the peak value, as well as the appearance of secondary peak, in the PSD curves was observed in specimens located near the perimeter of the sampler (including the top and bottom ends).

From a practical viewpoint, the examples described above suggest that, to obtain representative soil properties to be used in geotechnical design, fixed piston samplers should be always considered over Shelby tubes. The microstructural analysis described above showed that 50-mm Shelby tubes should be avoided in practice. Even if

the centreline of a 50-mm Shelby tube does not display important structural modifications (disturbance), extra caution should be taken if the diameter of the sample required for triaxial or oedometer testing is similar to the Shelby tube. Although the testing of small triaxial specimens is feasible, discarding the outer 4-mm annulus of soil implies that the tested specimen will include some material near the perimeter of the tube where important variations in soil fabric occur.

Acknowledgements This work in FEUP was supported by FCT by the project PTDC/ECM-Geo/1780/2014, Liquefaction Assessment Protocols to Protect Critical Infrastructures Against Earthquaker Damage, financed the European Communion Operational Program for Competitive Factors, COMPETE and developed under the activities of the Institute of R&D in Structures and Construction (CONSTRUCT). The first wants to thank Dr. Cristiana Ferreira for her continuous collaboration, as well as for the interaction with Dr. Mori, a recognized expert on the subject who has shared a lot of his knowledge for this work. The second author wants to thank Assoc. Prof. Marcos Arroyo and Núria Sau (UPC, Barcelona) as well as the Spanish Ministry of Science and IGEOTEST for the support provided through the research Project TRA2009_0076. The support provided by all contributing partners to the ARC Centre of Excellence for Geotechnical Sciences and Engineering at the University of Newcastle, Australia (Advanced Geomechanics, Coffey Geotechnics and Douglas Partners, and the NSW Science Leveraging Fund of NSW) is also acknowledged.

References

1. Andersen A, Kolstad P (1979) The NGI 54-mm samplers for undisturbed sampling of clays and representative sampling of coarser materials. In: Proc. Int. Symp. Soil Sampling, Singapore, pp 13–21
2. Ashi J (1997) Computed tomographic scan image analysis of sediments. In: Proc. Of the Ocean Drillings Program, Scientific Results, vol 156, pp 151–159
3. Arroyo M, Pineda JA, Sau N, Devicenzi M, Perez N (2015) Sample quality examination on silty soils. In: Geotechnical engineering for infrastructure and development. Institution of Civil Engineers, UK, pp 2873–2878. doi:10.1680/ecsmge.60678.vol6.445
4. ASTM D6519–08 (2008) Standard practice for sampling of soil using the hydraulically operated stationary piston sampler. ASTM International, West Conshohocken. http://www.astm.org
5. Baligh MM (1985) The strain path method. J Geotech Eng Div ASCE 111(GT9):1108–1136
6. Baligh MM, Azzouz AS, Chin CT (1987) Disturbance due to 'ideal' tube sampling. J Geotech Eng 113(7):739–757
7. Besenzon D (2013) The use of seismic waves for geotechnical characterization. MSc Thesis, Universitá Degli Studi di Padova, Facoltá de Ingegneria
8. Clayton CRI, Siddique A, Hopper RJ (1998) Effects of sampler design on tube sampler disturbance-numerical and analytical investigations. Geotechnique 48(6):847–867
9. Clayton CRI, Simons NE, Matthews MC (1995) Site investigation, 3rd edn. University of Surrey, United Kingdom
10. Cubrinovski M, Bradley BA, Wotherspoon L, Green RA, Bray JD, Wood C, Pender M, Allen J, Bradshaw AS, Rix G et al (2011) Geotechnical aspects of the 22 February 2011 Christchurch earthquake. Bull N Z Soc Earthq Eng 44(4):205–226
11. DeGroot DJ, Ladd CC (2012) Site characterization for cohesive soil deposits using combined in situ and laboratory testing. In: Rollins K, Zekkos D (eds) Geotechnical Engineering State of the Art and Practice: Keynote Lectures from GeoCongress 2012, Geotechnical Special Publication, 2012, No. 226. ASCE Geo-Institute, pp 565–608
12. Delage P, Lefebvre G (1984) Study of the structure of a sensitive Champlain clay and of its evolution during consolidation. Can Geotech J 21(1):21–35
13. Diamond S (1970) Pore size distributions in clays. Clays Clay Miner 18(1):7–23. doi:10.1346/CCMN.1970.0180103
14. Díaz JI, Ercilla G (1993) Holocene depositional history of the Fluviá—Muga prodelta, northwestern Mediterranean Sea. Mar Geol 111(1):83–92
15. Donohue S, Long M (2010) Assessment of samples quality in soft clay using shear wave velocity and suction measurements. Géotechnique 60(11):883–889
16. Duliu OG (1999) Computer axial tomography in geosciences: an overview. Earth Sci Rev 48:265–281
17. Dyvik R, Madhus C (1985) Laboratory measurements of Gmax using bender elements". In: Proceedings ASCE Annual Convention: Advances in the art of testing soils under cyclic conditions, Detroit, pp 186–197
18. Emdal A, Gylland A, Amundsen HA, Ksin K, Long M (2016) Mini-block sampler. Can Geotech J 53(8):1235–1245
19. Ferreira C (2009) The use of seismic wave velocities in the measurement of stiffness of a residual soil. PhD Thesis, University of Porto
20. Ferreira C, Mendonça AA, Viana da Fonseca A (2004) Assessment of sampling quality in experimental sites on residual soils from Porto granite. In: Proc. of the 9th Portuguese conference on geotechnics, vol 1. SPG, Lisbon, pp 27–38 **(in Portuguese)**
21. Ferreira C, Viana da Fonseca A, Nash D (2011) Shear wave velocities for sample quality assessment on a residual soil. Soils Found 51(4):683–692 **(Special Issue on "Deformation Characteristics of Geomaterials", Elsevier)**
22. Gasparre A, Hight DW, Coop MR, Jardine RJ (2014) The laboratory measurement and interpretation of the small-strain stiffness of stiff clays. Géotechnique 64(12):942–953. doi:10.1680/geot.13.P.227
23. Gimias (2011) Graphical interface for medical image analysis and simulation, Gimias_v1.2.0. Centre for Computational Image and Simulation Technologies in Biomedicine (CISTIB)/Universitat Pompeu Fabra (UPF), Barcelona. http://www.gimias.org
24. Hight DW (1986) Laboratory testing: assessing BS 5930. In: Proc. 20th regional meeting of the Engineering Group of the Geological Society, University of Surrey, pp 43–52
25. Hight DW, Boese R, Butcher AP, Clayton CRI, Smith PR (1992) Disturbance of the Bothkennar clay prior to laboratory testing. Géotechnique 42(2):199–217
26. Huang AB, Tai YY, Lee WF, Ishihara K (2008) Sampling and field characterization of the silty sand in Central and Southern Taiwan. In: 3rd international conference on site characterization (ISC-3), Taipei. Taylor & Francis, pp 1457–1463
27. Hvorslev MJ (1949) Subsurface exploration and sampling of soil for civil engineering purposes U.S. Army Corps of Engineers, Vicksburg
28. Idriss IM, Boulanger RW (2008) Soil liquefaction during earthquakes. In: Earthquake Engineering Research Institute (EERI), Oakland
29. ISSMGE, International Society of Soil Mechanics and Foundation Engineering (1981) Manual for the sampling of soft cohesive soils, ISSMFE Sub-committee on Soil Sampling. Japanese Geotechnical Society, p 129
30. Ismail MA, Rammah KI (2005) Shear-plate transducers as a possible alternative to bender elements for measuring G_{max}. Géotechnique 55(5):403–407

31. Jamiolkowski M (2014) Geotechnical characterization of a tailings deposit in Poland—an update. In: Proc. 3rd Int. Symp. Cone Penetration Testing, Las Vegas
32. Jamiolkowski M, Masella A (2015) Geotechnical characterization of copper tailings at Zelazny Most Site. In: Marchetti, Monaco, Viana da Fonseca (eds) Keynote Lecture, DMT'15 The 3rd Int. Conf. on the Flat Dilatometer, Rome, pp 25–42. ISBN 979-12-200-0116-8
33. Kazuo T, Kaneko S (2006) Undisturbed sampling method using thick water-soluble polymer solution Tsuchi-to-Kiso. J Jpn Geotech Soc 54(4):145–148 **(in Japanese)**
34. Kelly RB, Pineda JA, Bates L, Suwal L, Fitzallen I (2017) Site Characterisation for the Ballina Field Testing Facility. Géotechnique 67(4):279–300
35. Krage C, Albin BM, DeJong JT, DeGroot D (2016) The influence of in situ effective stress on sample quality for intermediate soils. In: Proc. 5th international conference in geotechnical and geophysical site characterization, ISC'5
36. Ladd CC, Lambe TW (1963) The strength of undisturbed clay determined from undrained tests. In: Symp. on laboratory shear testing of soils, ASTM, pp 342–371
37. Ladd CC, DeGroot DJ (2003) Recommended practice for soft ground site characterization. In: The Arthur Casagrande Lecture, 12th Pan. Conf. on Soil Mech. and Geotech. Eng., MIT, vol 1, pp 3–57
38. Landon MM, DeGroot DJ, Sheahan TC (2007) Non-destructive sample quality assessment using shear wave velocity. J Geotech Geoenviron Eng 133(4):424–432
39. La Rochelle P, Sarrailh J, Tavenas F, Roy M, Leroueil S (1981) Causes of sampling disturbance and design of a new sampler for sensitive clays. Can Geotech J 18(1):52–66
40. Lee WF, Ishihara K, Chen CC (2012) Liquefaction of silty sand—preliminary studies from recent Taiwan, New Zealand and Japan earthquakes. In: Proc. Int. Symp. Engineering lessons learned from the 2011 Great East Japan Earthquake, Tokyo
41. Lefebvre G, Poulin C (1979) A new method of sampling in sensitive clay. Can Geotech J 16:226–233
42. Lo Presti DCF (1995) General report: measurement of shear deformation of geomaterials in the laboratory. In: Shibuya, Mitachi, Miura (eds) Pre-failure deformation of geomaterials. Balkema, Rotterdam, pp 1067–1088
43. Lunne T, Berre T, Strandvik S (1997) Sample disturbance effects in soft low plasticity Norwegian clay, Recent developments in soil and pavement mechanics. Balkema, Rio de Janeiro, pp 81–92
44. Mathijssen FAJM, Boylan N, Long M (2008) Sample disturbance of organic soils. In: Huang, Mayne (eds) Proc. geotechnical and geophysical site characterization, pp 1481–1488
45. Marcuson WF, Franklin AG (1979) State of the art of undisturbed sampling of cohesionless soils. Miscellaneous Paper—US Army Engineer Waterways Experiment Station, (GL-79-16)
46. Markham CS, Bray JD, Riemer MF, Cubrinovski M (2016) Characterization of shallow soils in the central business district of Christchurch, New Zealand. Geotech Test J 39(6):922–937. doi:10.1520/GTJ20150244
47. Mitchell JK (1976) Fundamentals of soil behaviour. Wiley
48. Mori K, Sakai K (2016) The GP sampler: a new innovation core sampling. Aust Geomech 51(4):131–166 **(ABN 89 615 696 393. Sydney)**
49. Nash DFT, Lings ML, Benahmed N, Sukolrat J, Muir Wood D (2006) The effects of controlled destructuring on the small strain shear stiffness Go of Bothkennar clay. In: Ling, Callisto, Leshchinsky, Koseki (eds) Geomechanics: laboratory testing, modeling and applications. A coll of papers of the geotech symposium in Rome
50. Ng CWW, Wang Y (2001) Field and laboratory measurements of small strain stiffness 503 of decomposed granites. Soils Found 41(3):57–71
51. Ng CWW, Leung EHY (2007) Determination of shear–wave velocities and shear moduli of completely decomposed tuff. J Geotech Geoenviron Eng ASCE 133(6):630–640
52. Ng CWW, Leung EHY, Lau CK (2004) Inherent anisotropic stiffness of weathered geomaterial and its influence on ground deformations around deep excavations. Can Geotech J 41(1):12–24
53. Orsi TJ, Anderson AL (1999) Bulk density calibration for X-ray tomographic analyses of marine sediments. GeoMar Lett 19:270–274
54. Osterberg J (1973) An improved hydraulic piston sampler. In: Proc. 8th Int. Conf. Soil Mech. and Foundation Eng, vol 1.2, pp 317–321
55. Pineda JA, Arroyo M, Sau N, Pérez N, Gens A (2012) Testing block samples from silty deposits. In Coutinho, Mayne (eds) ISC4, Porto de Galinhas. Taylor & Francis Group, Brazil, pp 1815–1823
56. Pineda JA, McConnell A, Kelly RB (2014) Performance of an innovative direct-push piston sampler in soft clay. In: Proc. 3rd symposium on cone penetration testing, CPT14, Las Vegas, CPT14 Press, pp 279–288
57. Pineda JA, Suwal LP, Kelly R (2014) Sampling and laboratory testing of Ballina clay. Aust Geomech 49(4):27–38
58. Pineda JA, Suwal L, Kelly RB, Bates L, Sloan SW (2016) Characterization of the Ballina clay. Geotechnique 66(7):556–577
59. Pineda JA, Liu XF, Sloan SW (2016) Effects of tube sampling in soft clay: a microstructural insight. Geotechnique 66(12):969–983
60. Rocchi I, Coop MR (2015) The effects of weathering on the physical and mechanical properties along a profile of a granitic saprolite. Géotechnique **(in press)**
61. Romero E (1999) Characterization and thermos-hydro-mechanical behaviour of unsaturated Boom clay: an experimental study. PhD Thesis, Universitat Politecnica de Catalunya, Barcelona
62. Sau N (2013) CAT scanner as a tool for geotechnical simple inspection. MSc Thesis, Department of Geotechnical Engineering and Geosciences, UPC, Barcelona
63. Sau N, Arroyo M, Perez N, Pineda JA (2015) Using CAT to obtain density maps in Sherbrooke specimens of silty soils. In: Soga, Kumar, Biscontin, Kuo (eds) International symposium on geomechanics from micro to macro, IS-Cambridge 2014. CRC Press, pp 1153–1158
64. Shibuya S (2000) Assessing structure of aged natural sedimentary clays. Soils Found 40(3):1–16
65. Singh S, Seed HB, Chan CK (1982) Undisturbed sampling of saturated sands by freezing. J Geotech Eng Div 108(GT2):247–264 **(ASCE)**
66. Stringer M, Beyzaei C, Cubrinovski M, Bray J, Riemer M, Jacka M, Wentz R (2015) Liquefaction characteristics of Christchurch silty soils: Gainsborough Reserve. In: 6th Int. conf. on earthquake geotechnical engineering, Christchurch
67. Stringer ME, Cubrinovski M, Haycock I (2016) Experience with Gel-Push sampling in New Zealand. In: Proc. 5th international conference in geotechnical and geophysical site characterization, ISC'5
68. Sukolrat J, Nash DFT, Benahmed N (2008) The use of bender elements in the assessment of disturbance of soft clay samples. In: Huang, Mayne (eds) Proc. geotechnical and geophysical site characterization, pp 1489–1495
69. Tan TS, Lee FH, Chong PT, Tanaka H (2002) Effect of sampling disturbance on properties of Singapore clay. J Geotech Geoenviron Eng 128(11):898–906
70. Tanaka H (2008) Sampling and sample quality of soft clays. In: Huang, Mayne (eds) Keynote lecture. Geotechnical and geophysical site characterization, pp 139–157

71. Tanaka H, Sharma P, Tsuchida T, Tanaka M (1996) Comparative study on sample quality using several types of samplers. Soils Found 36(2):57–68
72. Taylor ML, Cubrinovski M, Haycock I (2012) Application of new 'Gel-push' sampling procedure to obtain high quality laboratory test data for advanced geotechnical analyses. In: Proc. New Zealand Society of earthquake engineering conference, Paper No. 123, Christchurch
73. Terzaghi K, Peck R, Mesri G (1996) Soil mechanics in engineering practice. Wiley, New York
74. Viana da Fonseca A (1998) Identifying the reserve of strength and stiffness characteristics due to cemented structure of a saprolitic soil from granite. In: 2nd international symposium on hard soils—soft rocks, Naples, vol 1. A. A. Balkema, Rotterdam, pp 361–372
75. Viana da Fonseca A (2003) Characterising and deriving engineering properties of a saprolitic soil from granite, from Porto. In: Tan TS, Phoon KK, Hight D, Leroueil S (eds) Characterisation and engineering properties of natural soils, vol 2. Balkema, Swets & Zeitlinger, Netherlands, pp 1341–1378
76. Viana da Fonseca A, Coutinho RQ (2008) Characterization of residual soils. In: Huang A-B, Mayne P (eds) Geotechnical and geophysical site characterization. Balkema, Taylor & Francis Group, London, pp. 195–248. ISBN 978-0-415-46936-4
77. Viana da Fonseca A, Topa Gomes A (2010) Project and construction of Underground stations and tunnels (TBM and NATM) in heterogeneous masses for Metro do Porto. In: Aula PAYMACotas (ed) Excavations and tunnels in granite. Universitat Politècnicade Catalunya, Barcelona, pp 79–123
78. Viana da Fonseca A, Carvalho J, Ferreira C, Santos JA, Almeida F, Pereira E, Feliciano J, Grade J, Oliveira A (2006) Characterization of a profile of residual soil from granite combining geological, geophysical and mechanical testing techniques. Geotech Geol Eng 24(5):1307–1348
79. da Fonseca Viana, Ferreira C, Fahey M (2009) A framework interpreting bender element tests, combining time-domain and frequency-domain methods. Geotech Test J 32(2):1–17
80. Viana da Fonseca A, Coop M, Fahey M, Consoli N (2011) The interpretation of conventional and non-conventional laboratory tests for challenging geotechnical problems, deformation characteristics of geomaterials. IOS Press, Amsterdam, pp 84–119
81. Viana da Fonseca A, Amaral MF, Panico F, Rios S (2014) Indexation of dynamic and static geomechanical properties of a cemented aggregate for transportation engineering. J Transp Geotech 1:31–44 **(Elsevier)**
82. Washburn EW (1921) Note on a method of determining the distribution of pore sizes in a porous material. Proc Natl Acad Sci USA 7:115–116
83. Yanagisawa N, Kaneko S, Tani K, Sakai K (2004) Experimental study on a new method of undisturbed sampling using high-concentration water-soluble polymer. In: 32nd symposium on rock mechanics, Japanese Soc. of Civil Engineering, pp 311–316 **(in Japanese)**
84. Yokoi Y, Sakai K, Yukawa H, Orihara K (2015) Application of gel-push (GP) sampling method to slaking prone residual soil and reclaimed sand in Singapore. In: Proceedings of international conference on soft ground engineering, Singapore